TEMPERATURE, STRAIN RATE AND ANISOTROPY EFFECTS ON COMPRESSIVE RESPONSE OF NATURAL AND SYNTHETIC CELLULAR CORE MATERIALS

Claudia Sergi[1,2*], Fabrizio Sarasini[1], Jacopo Tirillò[1], Enrique Barbero[2], Sonia Sanchez-Saez[2], Marco Sasso[3], Edoardo Mancini[4]

[1] Department of Chemical Engineering Materials Environment, Sapienza Università di Roma and UdR INSTM, Italy

[2] Department of Continuum Mechanics and Structural Analysis, Universidad Carlos III de Madrid, Spain

[3] Department of Industrial Engineering and Mathematical Sciences, Università Politecnica delle Marche, Italy

[4] Department of Industrial and Information Engineering and Economics, Università degli Studi dell'Aquila, Italy

*Corresponding author: claudia.sergi@uniroma1.it

ABSTRACT

The remarkable flexural properties of sandwich structures, which make them the first choice in many industrial fields, hinge on the selection of performing core materials with suitable out of plane mechanical properties. In light of this, the knowledge of cellular core materials compressive behaviour plays a major role during sandwich structure design. For this reason, this work provides a detailed comparison of the compressive behaviour between a synthetic foam (polyvinyl chloride) and an environmentally friendly agglomerated cork as a function of density, strain rate, temperature and anisotropy. The strain rate sensitivity of these cellular materials was investigated in a wide range of velocity conditions by using drop weight tower and Split Hopkinson Pressure Bar dynamic compression tests. The experimental results highlighted a remarkable strain rate sensitivity of both materials because of their viscoelastic nature and, in particular, an increase in compressive properties with increasing strain rate. This increment turns out to be more pronounced in the medium-high strain rate range (approx. 80-250 1/s for agglomerated cork and 110-900 1/s for PVC foams) than in the low-medium one (approx. 0.001-80 1/s for agglomerated cork and 0.001-110 1/s for PVC foams). The experimental results also pointed out an embrittlement effect with decreasing temperature, which compromises core materials crashworthiness determining a reduction of the percentage absorbed energy, and a remarkable anisotropy induced by the production processes. The outcomes of the work confirm the feasibility of agglomerated cork as a sustainable alternative to petroleum-based cellular core materials especially in consideration of the remarkable recovery capabilities that ensure a higher dimensional stability of the sandwich structure.

Keywords: Agglomerated Cork, PVC Foam, Split Hopkinson Pressure Bar, Dynamic Compression, Strain Rate, Temperature

1 INTRODUCTION

Lightweight structures characterized by high stiffness and strength are highly needed in all industrial applications where the optimisation of mechanical performances and structure weight is the main goal. For this reason, in the last decades there was a widespread use of sandwich structures in many industrial fields such as automotive, marine, aeronautical, construction, aerospace, wind turbines and so on. This particular class of composites is characterized by impressive flexural properties that are reached thanks to the major role played by the core material that separates the skins, i.e. the load-bearing structures for in plane and bending loads [1]. In order to be efficient, a core material should meet the following requirements: low density, high shear properties and a high out of plane stiffness [2]. Considering the last feature, it appears as a direct consequence that the compressive behaviour of a core material is one of the main issues to take into account for material selection.

In light of this, one of the aims of this work is to provide a comprehensive investigation of the compressive behaviour of traditional synthetic polyvinyl chloride (PVC) foams over a wide range of strain rate conditions. Knowing how core compressive properties change as a function of strain rate is a key point to understand how the overall sandwich structure can react to an external load. Some studies already addressed in detail the quasi-static compressive properties of PVC foams relating their mechanical performances with their morphology [3,4], while others were focused on the strain rate dependency of PVC foam compressive properties [5–7]. Some of these research studies even took into account the effect of some important parameters such as density and microstructure [8,9] or temperature [10], but all of them considered quasi-static conditions and high velocity conditions completely neglecting the medium velocities. This means that core material behaviour in these loading conditions is still relatively unknown thus preventing the prediction of the resulting sandwich composite response and making difficult to ensure its feasibility in all those applications that may expose the structure to this type of dynamic stress. The importance of knowing foam behaviour at intermediate strain rates was demonstrated by many studies such as the ones proposed by Morton et al. [11], Chiacchiarelli et al. [12], Wouts et al. [13], Colombo et al. [14] and Zhai et al. [15]. Morton et al. studied the influence of low and intermediate strain rates on low density expanded polypropylene foams (EPP) and found out a significant increase in collapse stress, 45 % and 57 % depending on foam density, already in this limited working range. Wouts et al. addressed the strain rate sensitivity of two types of wood, spruce and beech, highlighting an increase in crushing and plateau stresses with increasing strain rates that becomes much more pronounced in the medium-high range. This means that a change in wood compressive response was detected depending on the strain rate range under consideration. Zhai et al. investigated the influence of strain rate on the Poisson's ratio of an auxetic polyurethane foam proving that the material displays an auxetic behaviour in the low-medium strain rate range but moves to a positive Poisson's ratio for higher strain rates. To bridge the gap on PVC medium strain rate conditions, this work covers the whole strain rate range through the help of quasi-static compression tests, drop weight tower and Split Hopkinson Pressure Bar dynamic compression tests. In this way it is possible to analyse the foam material behaviour in low, medium and high velocity conditions and to evaluate the evolution of its main compressive properties with test speed. All the tests were carried out on PVC foams with different densities in order to evaluate the effect of this paramount parameter on their compressive behaviour and their strain rate dependency. After this first section, the work examines in depth the effect of other critical parameters on PVC foams compressive behaviour. In particular, it deals with the combined effect of impact energy and low and high temperatures on PVC dynamic compression properties and with the effect of production process on PVC foams anisotropy.

Polymeric foams from crude oil, such as PVC, were extensively used throughout the years thanks to their satisfying mechanical properties that make them suitable as core materials, but the environmental concerns generated by pollution and by the ever-growing amount of waste to be disposed encouraged to find an eco-friendly alternative. To face the increasing restrictions imposed by the new regulations in the field of landfills, many research studies started to focus on the mechanical properties, and in particular the compressive properties, of bio-based cores such as balsa wood [7,16], natural cork [17–21] and agglomerated cork [22]. In view of this, the other main aim of this work is to propose a promising environmentally-friendly alternative to the commonly used synthetic foams. To reach this goal three agglomerated corks, which differ for density and granule size, were submitted to the same experimental campaign previously described for PVC. This choice not only ensures a complete analysis of the compressive behaviour of an innovative core material from renewable resources but also a full comparison with a more traditional synthetic foam.

It is necessary to consider that even for cork, many studies already addressed its dynamic compressive behaviour, but none of them provides a comprehensive overview on its compressive response in the whole range of strain rate conditions, as already highlighted for PVC. Sasso et al. [23] presented an exhaustive description of agglomerated cork strain rate sensitivity including the evaluation of local accelerations and consequently the inertia stresses through DIC analysis but considering only quasi-static and high velocity conditions. The same strain rate ranges were used by Gameiro et al. [24] who investigated natural, agglomerated and micro agglomerated cork dynamic compression behaviour. The medium velocity conditions were studied through drop weight tower tests by Sanchez-Saez et al. [25,26] who addressed the effect of thickness on the energy-absorption capabilities and the multiple impact resistance of agglomerated cork. The first two works disclosed a strong strain rate sensitivity of cork, mainly due to its viscoelastic nature, which induces an increase in its compressive properties moving from quasi-static conditions to high strain rate conditions, as previously observed for other polymeric foams. The other two works proves the high energy absorbing capabilities of agglomerated cork that, moreover, keep almost constant even after repeated impacts. The present work includes all the strain rate conditions proposed in the cited studies, ensuring a thorough analysis of the strain rate sensitivity along the whole dynamic working range. The use of agglomerated cork planks as core material allows to take advantage of all peculiar cork properties, such as stunning recovery capability, high fire resistance, excellent damping capability and good acoustic and thermal insulation capacities. Moreover, it permits to optimise the exploitation of waste from wine stopper manufacturers by keeping products and materials in use that otherwise would be disposed, in line with the principles of circular economy.

In this framework, the present work aims to provide a thorough overview of the compressive behavior of traditional PVC foams and of more innovative and eco-friendly agglomerated cork cores. Low, medium and high strain rate conditions were considered in order to follow compressive properties evolution throughout the whole working range (approx. 0.001-250 1/s for agglomerated cork and 0.001-900 1/s for PVC foams). This allows to overcome the lack of previous works, on both PVC foams and agglomerated corks, which addressed only one or two of the strain rate ranges preventing an overview of the overall compressive response. The analysis of cores compressive response is completed with the investigation of two others paramount factors: operating temperature and anisotropy. Drop weight tower dynamic compression tests allowed to investigate the combined effect of impact energy and extremely low (-40 °C) and high (60 °C) operating temperatures. These two parameters were addressed only separately for agglomerated cork in previous works [27,28] and were never addressed for PVC foams.

2 MATERIALS AND METHODS

2.1 Materials

Divinycell HP130, HP200 and HP250 are the three PVC foams selected for this research study. These core materials, provided by Diab®, are closed cell foams with an average density of 130 kg/m^3, 200 kg/m^3 and 250 kg/m^3, respectively. The rationale of this choice is dictated by the need to investigate the influence of this parameter on PVC compressive behaviour. The natural cellular core materials chosen to compare with Diab foams are three agglomerated corks that differ from one another in density and granule size. In order to provide a meaningful comparison of the compressive results obtained, the selected agglomerated corks have the same density values of the foams and in particular NL10 has an average density of 140 kg/m^3, NL20 of 200 kg/m^3 and NL25 of 250 kg/m^3. They were provided by Amorim Cork Composites® and are characterized by a grain size of 2-4 mm in the case of NL10 and a grain size of 0.5-2 mm in the case of NL20 and NL25. Cork granules are bonded together with a polyurethane binder specifically designed for cork that makes it compatible with all industrial resins. All core materials were supplied in the form of 15 mm thickness plates.

2.2 Quasi-static compression tests

Quasi-static compression tests were performed with a pneumatic testing machine model Si-plan® equipped with a 3 kN load cell. Core materials anisotropy was evaluated testing parallelepiped samples with a height of 15 mm and a square base of 12 mm of side. Tests were performed at three nominal strain rates, i.e. 10^{-3},10^{-1} and 10 s^{-1}, on samples cut with different orientations and in particular with the 15 mm side, that is the test direction, oriented along the three main axes of the planks, as represented in Figure 1. [A] samples allow to investigate the z axis compressive properties of the core materials, [B] samples the y axis properties and [C] samples the x axis properties. Cellular cores strain rate sensitivity was investigated through cubic samples of 12 mm of side that were tested along the z axis and at two nominal strain rates, i.e. 10^{-3} and 10^{-1} s^{-1}. At least three samples were tested in every experimental condition.

2.3 Drop weight tower dynamic compression tests

Drop weight tower dynamic compression tests were carried out on cubic samples of 15 mm of side in a drop weight tower Ceast Fractovis® equipped with a flat impactor of 58 mm of diameter and an overall mass of

4.134 kg. Strain rate effect was investigated subjecting the samples to different impact energies as summarized in Table 1. It is appropriate to highlight that dynamic compression tests do not work with a constant strain rate as quasi-static compression and this leads to the need to define a univocal criterion for strain rate identification. Considering that this type of test records impact velocity throughout all test time, it allows to obtain automatically the evolution of strain rate with time. For this reason, in this work every strain rate value was estimated calculating the mean of all strain rate values included between the impact starting point and the point where the compressive property of interest occurs. For instance, to evaluate the strain rate at 20 % of deformation, the average values of the strain rate from t = 0 s up to the time corresponding to 20 % of deformation are computed.

Dynamic compression tests were performed not only at room temperature but also at 60 °C and -40 °C in order to monitor the evolution of dynamic compression properties in a wide range of temperatures. It was possible to perform the tests at these temperatures thanks to a climatic test chamber equipped with both heaters and nitrogen cooling connectors. Samples were pre-conditioned for two hours at the operating temperature in order to ensure a uniform temperature profile inside the whole specimen. This part of the experimental campaign was carried out using 5 J, 7 J and 13 J impact energies in order to give information on the combined effect of temperature and impact energy. Tests performed at room temperature were recorded with a high-speed camera, Fastcam SA-Z by Photron®, for visual inspection of the progressive effect of the impact on the core material. This operation was not possible with the tests performed at 60 °C and -40 °C because of the climatic chamber that needed to be maintained closed in order to keep constant the temperature inside it. At least five samples were tested in every testing condition.

2.4 Split Hopkinson Pressure Bar dynamic compression tests

Dynamic compression tests were carried out by means of a Split Hopkinson Bar. The adopted apparatus is made up of three aligned bars named pre-stressed, input and output bars characterized by a diameter of 18 mm and a length of 3.0 m, 7.5 m and 4.0 m, respectively as shown in Appendix A (Figure A1) [29]. The pre-stressed bar is the section of the apparatus where the pressure wave used to plastically deform the samples is generated. The wave is produced inducing a sudden release of the elastic energy stored by the bar thanks to a static pre-loading generated through an electro-mechanical actuator. The energy release takes place when a sacrificial element placed between the actuator and the pre-stressed bar fails in shear. The input compressive wave obtained travels through the input bar at the sound speed of the bar material and is transmitted to the sample that is placed between the input and the output bars. While the sample is deformed with a high strain rate, the wave is partially transmitted to the output bar and partially reflected back into the input bar. The bars are designed to stay within their elastic limit, while the sample is likely to undergo large deformations. The strain induced by the incident $\varepsilon_i(t)$, reflected $\varepsilon_r(t)$ and transmitted $\varepsilon_t(t)$ waves is measured by foil strain gage rosettes placed on the input and output bars.
The signals obtained are used to compute the load at the first and second edge of the sample according to the equations:

$$P_I\,(t) = E_I \cdot A_I[\varepsilon_I(t) + \varepsilon_R(t)] \tag{1}$$

$$P_O\,(t) = E_O \cdot A_o[\varepsilon_T(t)] \tag{2}$$

where *E* is the elastic modulus and *A* the cross-section area of the bars. Equation (1) refers to the input bar (I) whereas equation (2) refers to the output bar (O). Once calculated the loads, the stresses can be determined dividing the load values obtained for the specimen cross section area. Even the velocity at the two edges of the sample can be computed through the following equations:

$$\dot{u}_I\,(t) = C_I[\varepsilon_I(t) - \varepsilon_R(t)] \tag{3}$$

$$\dot{u}_O\,(t) = C_O[\varepsilon_T(t)] \tag{4}$$

where C is the sound speed of the bar material. The integration of equation (3) and (4) allows to calculate the engineering strain experienced by the material according to equation (5) where L_s is the specimen length:

$$\varepsilon(t) = \frac{1}{L_s}\int_0^t [\dot{u}_I\,(t) - \dot{u}_O\,(t)]dt \tag{5}$$

The bars are designed to stay within their elastic limit, while the sample is likely to undergo large deformations. For this reason, the input and output bars are typically made of a high strength metallic material. However, when soft materials have to be tested, it is mandatory to enhance the system sensitivity, especially for the load measurement. For this reason, a polyethylene terephthalate (PET) output bar was used for testing both PVC foam and cork samples. Its reduced stiffness permitted to achieve measurable strains even with the low pressure waves transmitted in the tests.
The pre-stressed and input bars used for the tests on cork were also made of PET, whereas pre-stressed and input bars used for the tests on PVC foam were made of aluminum (AA7075T6). In this way, a good compromise was obtained, with reasonable impedance mismatch between bars and sample (in order to deform the sample) and acceptable signals amplitudes on both input and output bars.
Moreover, the adopted configurations permitted to reach higher strain rates than in drop tower tests and simultaneously guaranteed the dynamic equilibrium in the samples. Figure A2 of Appendix A show the forces at the two edges of the samples, as computed by (1) and (2), for the fastest tests on PVC foam (A) and agglomerated cork (B). It is noted that the two forces increase nearly simultaneously and with few oscillations, meaning that the samples are in equilibrium and inertia effects are negligible within the samples.
The average strain rates achieved in the tests on PVC foam are in the range 500-1000 s^{-1}, whereas the average strain rates achieved in the test on cork are in the order of 150-200 s^{-1}. These values are computed as the average strain rate. Figure A3 of Appendix A shows the engineering strain rate as a function of strain for the fastest tests on PVC foam and cork. It is observed that after an initial ramp, the strain rate is reasonably uniform during the deformation, with a final decrease due to material densification
It is necessary to highlight that due to the viscoelastic nature of PET, the travelling wave is submitted to an attenuation and dispersion and the elastic modulus E_O of the output bar, and consequently the sound speed C_O, are not exactly constant. For this reason the dedicated calibration shown in [30] and the postprocessing procedure shown in [31] have been carried out. In particular, the analytical procedure based on the wave propagation theory and implemented in Matlab® permits to numerically shift in backward or forward direction the waves measured at the rosettes location, thus computing as the waves would appear when they interact with the specimen. Tests were carried out on parallelepiped samples with a height of 15 mm and a square base of 12 mm of side and, as in the case of quasi-static compression tests, both strain rate and anisotropy effect were investigated using the same sample configuration previously introduced in Figure 1. At least three samples were tested in every operative condition.

3 RESULTS AND DISCUSSION

3.1 Strain rate effect along z axis: out of plane properties

PVC foams compressive behaviour is characterized by three main steps [3,4] as can be easily detected in the curves shown in Figure 2. The first part of the curve is a straight line that describes the elastic deformation of cell walls and that ends at the yielding point where cell collapse and material plastic deformation begin. The second part of the curve is the plateau region that is characterized by an almost constant stress and describes the progressive buckling and collapse of the foam cells. This step ends when material densification occurs because of cell walls interaction. When foam cell walls start to touch each other, there is a strong increase in the stress that must be applied to continue deforming the polymeric foam. The densification step can be easily detected in the stress-strain compressive curve thanks to a steep increase in curve slope, but if this stage can be easily recognized, the densification stress, that is the stress value at which densification starts, is difficult to identify unequivocally. To overcome this problem, Avalle et al. [32] proposed a satisfying method that allows to calculate precisely and univocally the densification stress value. A good energy absorbing material has to dissipate the impact energy keeping small the reaction force exerted. A good parameter to evaluate the energy absorbing capacities of a material is the efficiency that is defined as the ratio between the energy absorbed by the material up to a strain ε and the stress σ itself, as reported in the following equation:

$$Efficiency = \frac{\int_0^{\varepsilon} \sigma(\varepsilon) d\varepsilon}{\sigma} \tag{6}$$

Plotting the efficiency as a function of stress, the curve obtained is characterized by a maximum peak, which is ascribed to the fact that beyond the densification stress the increase in absorbed energy becomes much lower than the corresponding increase in stress thus leading to a decrease in material absorbing efficiency. A typical efficiency stress curve is shown in in Appendix A (Figure A4). In light of this, it appears evident that the stress value at which the efficiency reaches the maximum value can be identified as the densification stress. For what concerns PVC foams dynamic compressive curves, it is of main importance to highlight that it was necessary to proceed with a signal processing because of the large oscillations in the registered force due to the inevitable mechanical waves reflection of drop weight systems. Locally estimated scatterplot smoothing (LOESS) was selected as smoothing tool to obtain reliable results. The smoothing process allows to obtain a much clearer and well-defined curve that traces accurately the original curve especially in correspondence of the peak value. This part of the curve is the one that has the main importance to reach a good precision of the densification stress value calculated.

The knowledge of densification stress and, as a consequence, densification strain allows to calculate accurately also the plateau stress. Indeed, the latter can be calculated according to equation (7):

$$\sigma_{pl} == \frac{\int_{\varepsilon_{cr}}^{\varepsilon_{dens}} \sigma(\varepsilon)\, d\varepsilon}{\varepsilon_{dens} - \varepsilon_{cr}} \tag{7}$$

where ε_{dens} is the densification strain and ε_{cr} is the strain corresponding to the base of the collapse stress peak.

The curves in Figure 2 allow also to identify a strong dependency of foam compressive properties on density and in particular the higher the density, the higher the yielding point and the plateau stress. Clearly an increase in foam density entails an increase in cell walls thickness thus improving their resistance against buckling [3,4].

Many studies already proved the strain rate sensitivity of PVC foams [5–8,10] demonstrating that the higher is the test speed, the higher the plateau stress and the yielding point will be. The results obtained in this work are in perfect agreement with the ones of previous works, in fact when strain rate increases compressive curves tend to shift upwards as it is possible to observe from the HP200 curves represented in Figure 3. What is of main interest is that the dynamic compressive curves obtained in medium velocity conditions fit perfectly the blank space between quasi-static compressive curves and Split Hopkinson Pressure Bar curves. It is also worthwhile to underline that drop weight tower dynamic compressive curves show a different shape with respect to quasi-static and Split Hopkinson Pressure Bar ones. If these last two appear as open lines, drop weight tower curves present a closed loop because the tests carried out allow to record material reaction force even in the impactor rebound stage thus permitting to detect the unloading phase of the sample.

A deeper understanding of the results is possible through the analysis of the data plotted in Figure 4 that represent the plateau stress and the densification stress of the PVC foams under study against strain rate in logarithmic scale. In quasi-static conditions there is only a slight increase in plateau and densification stress until medium velocity conditions are reached. Once in these conditions, a strong increase in plateau stress is observed with greater improvements corresponding to increasing density. The dependence of PVC foams compressive properties on strain rate has to be ascribed to their viscoelastic nature that plays an ever more important role when foam density and polymer content increase.

Moving to the more innovative and eco-friendly agglomerated cork, the curves in Figure 5 underline a different compressive behaviour with respect to PVC foams that can be ascribed to the pronounced difference in cell walls morphology and chemical composition. PVC cell walls are straight and rigid and tend to fracture and collapse when the critical stress is reached, instead cork ones exhibit undulations that permit to adapt to the applied deformation without undergoing fracture. This ability of cork cell walls to intensify their corrugation when material deformation increases is due to the suberin, a glyceridic polyester with a ribbon like structure [17,19]. Agglomerated cork curves are characterized by three main regions: a first elastic region where cell walls bend elastically, a second broad plateau region were cells buckle and corrugate without undergoing fracture and a final region of densification. It is necessary to highlight that agglomerated cork plateau region is characterized by a slight slope that causes a progressive increase of plateau stress with increasing strain. In light of this, agglomerated cork plateau stress was not calculated according to equation (7) but two different values at 20 % and 30 % of deformation where considered in order to take into account and highlight this feature of the bio-based cellular core. As previously detected for PVC foams, even in this case a sharp dependency of agglomerated cork compressive properties on density can be observed.

Even agglomerated cork displays a strong strain rate sensitivity as it is possible to infer from the curves represented in Figure 6, from the data plotted in Figures 7 and 8 and in agreement with the results presented in previous research studies [23,24]. Also for agglomerated cork, it is noteworthy how drop weight tower dynamic compressive curves fit perfectly the blank space left between quasi-static compression curves and Split Hopkinson Pressure Bar curves ensuring the filling of the gap of knowledge in the medium velocities range.

Figure 7 presents the tendency of plateau stress at 20 % and 30 % of deformation of the three agglomerated corks against strain rate in logarithmic scale, whereas Figure A5 in Appendix A depicts the same tendency but for the densification stress. If the medium-high velocity range shows a tendency of cork compressive properties that is totally comparable with PVC foam ones, the results seem to differ slightly in the low-medium velocity range. In the upper strain rate conditions, a sharp increase in plateau and densification stress can be detected for both classes of core materials, but in the lower strain rate conditions PVC foams display a much lower percentage increase in plateau and densification stress values when compared to agglomerated cork. As a matter of fact, agglomerated cork shows an increase of both plateau and densification stress between 40 % and 60 % whereas PVC foam only a 13 % increase. This marked difference in compressive properties can be explained considering that PVC foams have intrinsically higher mechanical properties than agglomerated cork ones.

These results are corroborated by the strain rate sensitivity analysis. Usually, strain rate sensitivity can be calculated plotting the evolution of the logarithm of the parameter under study (yielding point, plateau stress, densification stress, etc.) against the logarithm of the corresponding strain rate and computing the slope of the interpolation line. In the present study the sudden change in core materials behavior moving from the low-medium strain rate range to the medium- high one leads to the identification of two different interpolation lines and, as a consequence, to two different strain rate sensitivity values as also confirmed by the two exemplifying plots shown in Figure A6 of Appendix A. Agglomerated corks display a strain rate sensitivity between 0.029 and 0.041in the first segment and between 0.26 and 0.34 in the second one whereas PVC foams show a strain rate sensitivity between 0.009 and 0.026 in the first segment and between 0.16 and 0.27 in the second one. Both materials show a difference of one of order of magnitude moving from the low-medium to the medium-high strain rate range and from the data reported is possible to confirm the difference between agglomerated cork and PVC foams in the low-medium range. The change observed in strain rate sensitivity, moving from the low-medium range to the medium-high one, is in perfect agreement with the results achieved in other studies carried out on spruce and beech woods [13], but also on metals such as a ultrafine-grained alloy Ti-6Al-4V [33]. In conclusion, the introduction of the medium strain rate data allowed to detect the sharp change in curve slope going from the low- medium strain rates to the medium-high strain rates highlighting a transition that otherwise would have been lost.

3.2 Temperature effect

The evolution of cellular cores dynamic compressive properties in a wide range of temperatures was examined by performing tests at room temperature, 60 °C and -40 °C. Previous works addressed the effect of both high and low temperatures on agglomerated and expanded cork dynamic compressive behaviour but considering only a single impact energy [27,28]. In this work the combined effect of temperature and impact energy was evaluated through tests performed at 5 J and 7 J on all core materials and at 13 J for all PVC foams and NL25 agglomerated cork. A similar experimental campaign was carried out by Ptak et al. [34] who studied the effect of temperature and impact velocity on agglomerated and expanded cork through a hemispherical impactor. The study proposed by Ptak et al. addressed only the effect of a temperature higher than room temperature (50 °C) unlike this work that focuses also on temperature lower than room one. Moreover, the use of a hemispherical impactor does not allow to obtain a uniaxial compression in contrast to the flat impactor employed in this work that ensures a more homogeneous and uniform distribution of the compressive stress throughout the sample tested.

At first, the sole effect of energy was considered examining the results at room temperature. Figures 8 and 9 summarize the maximum force, maximum displacement and percentage absorbed energy values of all core materials subjected to 7 J and 13 J impacts at room temperature, respectively. The results of the 5 J impact are not reported because show the same tendency observed for the 7 J impact. This last confirms the remarkable absorbing capabilities of both PVC foams and agglomerated corks that are characterized by a percentage absorbed energy of almost 100 % and 98 %, respectively. For both core types maximum displacement tends to decrease when core density increases; in fact on equal impact energy conditions it is easier to deform a material with thinner cell walls. In particular, for a 5 J impact there is a difference of 24.21 % between NL10 and NL25 maximum displacement and a difference of 52 % between HP130 and HP250 whereas for a 7 J impact the difference is 11.63 % between NL10 and NL25 and 59.3 % between HP130 and HP250. The compressive behaviour of the two cellular materials tends to differ when maximum force values are analysed. For a 7 J impact, agglomerated cork maximum force increases when plank density decreases whereas PVC foam one displays the opposite trend. This happens because the two materials are working in two different compressive regions. Agglomerated cork has already reached the densification region where for small increases of displacement a strong increase in stress is observed. Considering that NL10 reaches a maximum displacement higher than NL25, it appears clear that it will also display a higher maximum force. On the contrary, all PVC foams are still working in the plateau region and this means that the maximum force depends on the foam yielding point that increases with increasing foam density.

Moving to the 13 J impact, it is necessary to highlight that NL10 and NL20 were not tested at this impact energy because the maximum deformation reached would have led to a maximum force too high and too close to load cell operating limit that could have compromised apparatus integrity and functionality. However, the tests carried out on NL25 highlight that its absorbing capacity is still comparable with PVC foams one. The maximum displacement results show the same tendency observed for the 7 J impact, but some differences are observable in PVC foams maximum force trend. HP130 maximum force seems almost equal to HP200 one because the foam with the lowest density is approaching the densification region.

Even if PVC foams are characterized by better mechanical performances than agglomerated corks thus being able to tolerate higher impact energies, the use of high-speed camera allowed to point out the main advantage of agglomerated cork over PVC, i.e. its dimensional recovery capability. NL25 (A) and HP130 (B) samples before and after a 13 J impact are represented in Figure 10. Even if the two materials undergo almost the same maximum deformation, 12 mm in one case and 13 mm in the other one, after almost 10 ms from the impact, NL25 has almost recovered its initial dimension whereas HP130 displays a halving of its initial height.

After this overview on core materials drop weight tower dynamic compressive behaviour at room temperature, it is possible to analyze the combined effect of temperature and impact energy. Maximum force and maximum displacement values at different operating temperatures for all core materials after a 5 J impact are summarized in Figure 11. An increase in maximum displacement can be observed for all cellular cores when operating temperature increases, in fact the lower the temperature the more brittle the compressive behaviour. Even in this circumstance natural and synthetic materials compressive behaviour tends to diverge when maximum force values are analysed. In the case of PVC foams, the maximum force value is reached at the yielding point and in the plateau region as demonstrated by the compressive curves depicted in Figure 12. This means that this parameter will depend on material strength that clearly increases when operating temperature decreases.

The results are a bit more scattered when agglomerated cork is under study. NL10 and NL20 show an increase in maximum force when operating temperature increases because at the higher temperatures they have already entered the densification region as demonstrated by the compressive curves in Figure 13. On the contrary, NL25 did not reach the densification region yet and behaves like PVC foams. This means that its maximum force is reached in the plateau region that is characterized by a higher stress when operating temperature is lower as shown in Figure 13.

7 J impact results are summarized in Figure 14 and it is possible to notice that the results are almost equal to the ones obtained at 5 J and that the only difference detected is in NL25 maximum force. The denser agglomerated cork reached the densification region, as demonstrated also by the compressive curves in Figure A7 in Appendix A, and so the maximum force value is not dictated by the plateau stress anymore thus leading to a compressive behaviour that is perfectly coherent with the one of NL10 and NL20.

Finally, for the 13 J impact results in Figure 15 a change in HP130 maximum force behaviour can be detected. In all three temperature conditions, the foam reaches densification but, in this region, a small increase in displacement leads to a high increase in stress and considering that the maximum displacement at 60 °C is much higher than the one at -40 °C, as shown in Figure A8 of Appendix A, this allows to explain the increase of maximum force with operating temperature.

The percentage absorbed energy results in Figure 16 show that absorbing energy capacity keeps almost constant with impact energy for all materials, but it decreases when operating temperature decreases. A more brittle behaviour caused by the reduction of materials movement at the molecular scale weakens their capacity to adapt to deformation and to dissipate energy in a viscoelastic way increasing strongly the elastic absorption component.

The embrittlement effect of temperature on agglomerated cork is also evident considering the damaging mode of NL10 and NL20 samples tested at -40 °C, as shown in Figure A9 of Appendix A. A visible detachment of a piece of the sample can be detected and it is mainly due to an intergranular fracture caused by the transition of the polymeric binder from the viscoelastic state to the glassy state. Indeed some previous studies demonstrated that the polyurethane binder glass transition temperature is at around -45 °C [35]. The embrittlement effect proved to be less pronounced on PVC foams because they keep the same behaviour and the same damaging mode over the whole temperature range having a glass transition temperature at around 85-90 °C [36] and working always in the glassy state.

3.3 Anisotropy effect

Polymeric foams anisotropy was extensively investigated over the years [37] whereas agglomerated cork mechanical performances are considered almost isotropic thanks to the random orientation of its granules that counteracts the intrinsic anisotropy of natural cork that displays different compressive performances along the three main directions [17]. In this work core materials anisotropy was investigated as a function of strain rate. In Figures 17 and A10 in Appendix A PVC foams plateau stress and densification stress in the three axis directions are represented as a function of strain rate. The results obtained confirm that the two in-plane stresses values (x axis [C] and y axis [B]) are almost equal and superimposable for the three foams whereas the out of plane stress (z axis [A]) is much higher. This anisotropy in compressive properties has to be ascribed to the production process that inflating gas through the polymeric mass leads to the formation of elongated cells along the z axis that look almost circular if observed perpendicularly to the x-y plane. Such arrangement of the cells makes denser the planes parallel to the z axis because of the presence of numerous and thicker cell walls that makes the material stiffer and stronger along the out of plane direction [38]. This hypothesis seems to be corroborated by the fact that the difference between in-plane and out of plane stress values is higher for lower foam density, in fact plateau stress values vary between 95-100 % for HP130, 65-80 % for HP200 and 55-60 % for HP250. It appears evident that the higher the amount of air trapped in the foam the higher the discrepancy in cell walls arrangement. PVC foam strain rate sensitivity along the z axis was extensively examined in the previous section, but from the results presented in Figures 17 and A7 it is possible to conclude that even the in-plane stress values are strain rate sensitive.

Figures 18, 19 and 20 report the plateau stress values at 20 % and 30 % of deformation and the densification stress values of NL10, NL20 and NL25, respectively. For NL10 it is possible to observe an isotropic behaviour since the plateau stress and densification stress values are equal irrespective of the compressive direction. This seems to confirm that the random orientation of cork granules allows to obtain almost an isotropic material. The situation changes when NL20 and particularly NL25 data are analysed. In fact, a certain difference between in-plane stress values and out of plane stress values can be observed. Contrary to what has been seen for PVC foams, out of plane stress in NL20 and NL25 agglomerated cork is characterized by a lower value than in-plane stresses.

Even in this case, the cause of the anisotropy has to be researched and attributed to the production process. Agglomerated cork planks are produced mixing cork granules with a polyurethane binder and submitting the mixture to heating and to a moderate pressure that tends to compress cork particles inducing residual stresses and causing a partial densification of the material [19]. Considering that the higher the density the earlier the agglomerated cork enters the densification region [22], it appears evident that the same operating pressure will induce in NL25 a greater amount of residual stresses along the z axis. This can lead to a more pronounced difference in NL25 in-plane and out of plane compressive properties than in NL20 or NL10 ones that appear even isotropic. Considering that the particles random orientation would lead to an isotropic material if the production process effect could be neglected, it is not surprising that agglomerated corks compressive properties display strain rate sensitivity regardless of the compressive direction, as previously shown even for PVC foams.

3.4 Results summary: comparison of the synthetic and bio-based cellular core materials.

The analysis of the compressive behavior of the synthetic PVC foams and of the natural agglomerated corks as a function of strain rate, operating temperature and anisotropy, pointed out some interesting findings.

For what concerns the strain rate effect, both PVC foams and agglomerated corks displayed a strong dependency on this parameter mainly due to their viscoelastic nature and, in particular, an increase in compressive properties was detected for increasing strain rates. This increase turned out to be much more pronounced in the medium-high velocity range for both core types. In the low medium range the increase in compressive properties was less marked in particular for the PVC foams and this is mainly due to their intrinsic higher mechanical properties.

It appears evident that the inherent higher mechanical performances of the PVC foams can guarantee higher flexural properties to the sandwich structures produced with them, but it must be considered that sandwich flexural properties depend also on skin distancing. A reduction of skin spacing during sandwich composite life cycle could determine a significant decrease in the flexural properties of the structure leading to an untimely failure of the component. Considering the remarkable recovery capabilities of agglomerated cork, it appears clear that it is able to guarantee a more constant spacing of the skins and as a consequence of the flexural performances of the structure throughout the working life. Moreover, the maintenance of the original shape plays a major role in structures such as wind turbine blades where change of the air flow on the blade could reduce the conversion efficiency of wind power in electrical energy.

Even if it is true that in principle PVC foams are characterized by higher mechanical properties than the agglomerated corks with the corresponding density, it is mandatory to highlight that NL25 displays performances that are totally comparable with HP130 ones. NL25 is characterized by a higher density than HP130, causing a slight increase in the weight of the sandwich structure produced with it, but it allows to obtain a much more eco-friendly composite with an improved biodegradability and this is an incomparable advantage for all those structures that can tolerate a little increase of their weight without major consequences. Moreover, the remarkable recovery capability makes it the preferred choice in all those applications where a multiple impact events resistance and efficiency are required.

Operating temperature is another key parameter that strongly influences both petroleum-based and bio-based cellular cores. A decrease in the working temperature leads to a decrease in materials maximum displacement thus highlighting a more brittle behaviour of the cores. This conclusion is also confirmed by the analysis of the percentage absorbed energy values that at equal impact energy tend to decrease at lower operating temperature. This means that a decrease in operating temperature can compromise the crashworthiness properties of the materials under study causing a decrease in absorbing capacity and an increase in plateau stress that in most cases results in an increase in maximum force reached.

4 CONCLUSIONS

The compressive behaviour of synthetic PVC foam cores was addressed taking into account several parameters such as density, strain rate, operating temperature and anisotropy. The same characterization was carried out on a natural cellular material in order to provide a bio-based alternative to the polymeric foams produced from crude oil. Agglomerated cork feasibility as core material in the production of sandwich structures was deeply investigated evaluating its out of plane properties as a function of the parameters previously cited. From the experimental results, the following conclusions can be drawn:

- strain rate strongly influences both PVC foams and agglomerated corks, because of their viscoelastic nature, determining an increment of their compressive properties;
- the most significant increase in the compressive properties was detected in the high-medium strain rate range whereas a slower increase was observed in the low-medium velocity;
- a decrease in operating temperature determines a decrease of maximum displacement and percentage absorbed energy for all core materials underlining an embrittlement effect and jeopardizing their crashworthiness with a decrease of their absorbing capacities;
- production process significantly contributes to induce anisotropy in all core material compressive properties;
- PVC foams production process induces an increase in its out of plane properties thanks to cell walls elongation along the z axis;
- agglomeration process causes a decrease of agglomerated corks out of plane properties because of the presence of residual stresses that are more pronounced for the denser cork.

APPENDIX A

REFERENCES

[1] Vinson R. J. The behavior of sandwich structures of isotropic and composite materials. Technomic publishing CO.,INC.; 1999.

[2] D. Zenkert. The handbook of sandwich construction. Engineering Materials Advisory Services Ltd; 1997.

[3] Lim GT, Altstädt V. Understanding the Compressive Behavior of Linear and Cross-linked Poly(vinyl chloride) Foams. J Cell Plast 2009;45:419–39. doi:10.1177/0021955X09105372.

[4] Colloca M, Dorogokupets G, Gupta N, Porfiri M. Mechanical properties and failure mechanisms of closed-cell PVC foams. Int J Crashworthiness 2012;17:327–36. doi:10.1080/13588265.2012.661637.

[5] Daniel IM, Cho J-M. Strain-Rate-Dependent Behavior of Polymeric Foams. 52nd AIAA/ASME/ASCE/AHS/ASC Struct. Struct. Dyn. Mater. Conf., 2011, p. 1–8.

[6] Mines RAW. Strain rate effects in crushable structural foams. Appl Mech Mater 2007;7–8:231–6. doi:10.4028/www.scientific.net/AMM.7-8.231.

[7] Tagarielli VL, Deshpande VS, Fleck NA. The high strain rate response of PVC foams and end-grain balsa wood. Compos Part B Eng Part B 2008;39:83–91. doi:10.1016/j.compositesb.2007.02.005.

[8] Saha MC, Mahfuz H, Chakravarty UK, Uddin M, Kabir E, Jeelani S. Effect of density , microstructure , and strain rate on compression behavior of polymeric foams. Mater Sci Eng A 2005;406:328–36. doi:10.1016/j.msea.2005.07.006.

[9] Wei Z, Nan Y. High strain rate and quasi-static compression behavior and energy absorption characteristic of PVC foam. Chall J Struct Mech 2016;2:212–5.

[10] Thomas T, Mahfuz H, Carlsson LA, Kanny K, Jeelani S. Dynamic compression of cellular cores : temperature and strain rate effects. Compos Struct 2002;58:505–12.

[11] Morton DT, Reyes A, Clausen AH, Hopperstad OS. Mechanical response of low density expanded polypropylene foams in compression and tension at different loading rates and temperatures. Mater Today Commun 2020;23. doi:10.1016/j.mtcomm.2020.100917.

[12] Chiacchiarelli LM, Cerrutti P, Flores-johnson EA. Compressive behavior of rigid polyurethane foams nanostructured with bacterial nanocellulose at low and intermediate strain rates. J Appl Polym Sci 2020;48701:1–13. doi:10.1002/app.48701.
[13] Wouts J, Haugou G, Oudjene M, Coutellier D, Morvan H. Strain Rate effects on the compressive response of wood and energy absorption capabilities - Part A : Experimental investigations. Compos Struct 2016. doi:10.1016/j.compstruct.2016.03.058.
[14] Colombo M, Martinelli P, Zedda R, Albertelli A, Marino N. Dynamic response and energy absorption of mineral – phenolic foam subjected to shock loading. Mater Des Des 2015;78:63–73. doi:10.1016/j.matdes.2015.04.014.
[15] Zhai X, Gao J, Liao H, Kirk CD, Balogun YA, Chen WW. Mechanical behaviors of auxetic polyurethane foam at quasi-static , intermediate and high strain rates. Int J Impact Eng 2019;129:112–8. doi:10.1016/j.ijimpeng.2019.03.002.
[16] Silva A Da, Kyriakides S. Compressive response and failure of balsa wood. Int J Solids Struct 2007;44:8685–717. doi:10.1016/j.ijsolstr.2007.07.003.
[17] Pereira H. The rationale behind cork properties: A review of structure and chemistry. BioResources 2015;10:1–23. doi:10.15376/biores.10.3.Pereira.
[18] Silva SP, Sabino MA, Fernandes EM, Correlo VM, Boesel LF, Reis RL. Cork: properties, capabilities and applications. Int Mater Rev 2008;53:256–256. doi:10.1179/174328008X353529.
[19] Knapic S, Oliveira V, Machado JS, Pereira H. Cork as a building material: a review. Eur J Wood Wood Prod 2016;74:775–91. doi:10.1007/s00107-016-1076-4.
[20] Anjos O, Rodrigues C, Morais J, Pereira H. Effect of density on the compression behaviour of cork. Mater Des 2014;53:1089–96. doi:10.1016/j.matdes.2013.07.038.
[21] Rosa ME, Fortes MA. Rate effects on the compression and recovery of dimensions of cork. J Mater Sci 1988;23:879–85. doi:10.1007/BF01153983.
[22] Jardin RT, Fernandes FAO, Pereira AB, Alves de Sousa RJ. Static and dynamic mechanical response of different cork agglomerates. Mater Des 2015;68:121–6. doi:10.1016/j.matdes.2014.12.016.
[23] Sasso M, Mancini E, Chiappini G, Sarasini F, Tirillò J. Application of DIC to Static and Dynamic Testing of Agglomerated Cork Material. Exp Mech 2018.
[24] Pires C, Jose GÆ. Experimental study of the quasi-static and dynamic behaviour of cork under compressive loading. J Mater Sci 2007;42:4316–24. doi:10.1007/s10853-006-0675-6.
[25] Sanchez-Saez S, García-Castillo SK, Barbero E, Cirne J. Dynamic crushing behaviour of agglomerated cork. Mater Des 2015;65:743–8. doi:10.1016/j.matdes.2014.09.054.
[26] Sanchez-Saez S, Barbero E, Garcia-Castillo SK, Ivañez I, Cirne J. Experimental response of agglomerated cork under multi-impact loads. Mater Lett 2015;160:327–30. doi:10.1016/j.matlet.2015.08.012.
[27] Kaczynski P, Ptak M, Wilhelm J, Fernandes FAO, Sousa RJA De. High-energy impact testing of agglomerated cork at extremely low and high temperatures. Int J Impact Eng 2019;126:109–16. doi:10.1016/j.ijimpeng.2018.12.001.
[28] Kaczynski P, Ptak M, Fernandes FAO, Chybowski L, Wilhelm J, Alves de Sousa RJ. Development and Testing of Advanced Cork Composite Sandwiches for Energy-Absorbing Structures. Materials (Basel) 2019;12. doi:10.3390/ma12050697.
[29] Mancini E, Sasso M, Rossi M, Chiappini G, Newaz G, Amodio D. Design of an Innovative System for Wave Generation in Direct Tension – Compression Split Hopkinson Bar. J Dyn Behav Mater 2015:201–13. doi:10.1007/s40870-015-0019-1.
[30] Martarelli M, Mancini E, Lonzi B, Sasso M. Sensor calibration of polymeric Hopkinson bars for dynamic testing of soft materials. Meas Sci Technol 2018;29.
[31] Sasso M, Antonelli M, Mancini E, Radoni M, Amodio D. Experimental and numerical characterization of a polymeric Hopkinson bar by DTMA. Int J Impact Eng 2017;103:50–63.
[32] Avalle M, Belingardi G, Montanini R. Characterization of polymeric structural foams under compressive impact loading by means of energy-absorption diagram. Int J Impact Eng 2001;25:455–72. doi:10.1016/S0734-743X(00)00060-9.
[33] Long YAN, Zhang W, Peng L, Peng H, Li X, Huang X. Mechanical Behaviors of Ultrafine-Grained Ti-6Al-4V Alloy During Compression at Various Strain Rates. Metall Mater Trans A 2020;51:4765–76. doi:10.1007/s11661-020-05895-x.
[34] Ptak M, Kaczynski P, Fernandes FAO, Alves de Sousa RJ. Assessing impact velocity and temperature effects on crashworthiness properties of cork material. Int J Impact Eng 2017;106:238–

48. doi:10.1016/j.ijimpeng.2017.04.014.
[35] Magalhães DPFD. Dynamic mechanical analysis and creep-recovery behavior of agglomerated cork. Eur J Wood Wood Prod 2017;0:0. doi:10.1007/s00107-017-1158-y.
[36] Jiang Z, Du Z, Xue J, Liu W, Li M, Tang T. Hierarchical structure and properties of rigid PVC foam crosslinked by the reaction between anhydride and diisocyanate 2018;46141:1–8. doi:10.1002/app.46141.
[37] Kanakkanatt S V. Mechanical Anisotropy of Open-Cell Foams. J Cell Plast 1972:50–3.
[38] Tita V, Caliri Junior MF. Numerical simulation of anisotropic polymeric foams. Lat Am J Solids Struct · 2012;1:1–21. doi:10.1590/S1679-78252012000200005.

Figures Captions

Figure 1: Orientations of the samples used to investigate a potential anisotropy of core compressive properties. The arrows show test direction and the respective property analyzed (in-plane/out-plane)

Figure 2: Effect of PVC foam density on 10^{-3} s^{-1} quasi-static compression curves

Figure 3: Effect of strain rate on HP130, HP200 and HP250 compressive behaviour

Figure 4: Average plateau stress and densification stress of the three types of PVC foam considered as a function of strain rate

Figure 5: Effect of agglomerated cork density on 10^{-3} s^{-1} quasi-static compression curves

Figure 6: Strain rate effect on the compressive behaviour of the three agglomerated corks under study (NL10, NL20 and NL25)

Figure 7: Average plateau stress at 20 % and 30 % deformation of the three agglomerated corks under study as a function of strain rate

Figure 8: Drop weight tower dynamic compression results of the six core materials subjected to a 7 J impact at room temperature: compressive curves, percentage absorbed energy, maximum force and maximum displacement

Figure 9: Drop weight tower dynamic compression results of the three PVC foams and of NL25 subjected to a 13 J impact at room temperature: compressive curves, percentage absorbed energy, maximum force and maximum displacement

Figure 10: NL25 (upper) and HP130 (lower) samples before and after almost 10 ms a 13 J impact

Figure 11: Maximum force and maximum displacement of all core materials at -40 °C, room temperature and 60 °C after a 5 J impact

Figure 12: Drop weight tower dynamic compressive curves of the HP130 core material submitted to a 5 J impact at the three operating temperatures

Figure 13: Drop weight tower dynamic compressive curves of NL10 and NL25 agglomerated corks submitted to a 5 J impact at the three operating temperatures

Figure 14: Maximum force and maximum displacement of all core materials at -40 °C, room temperature and 60 °C after a 7 J impact

Figure 15: Maximum force and maximum displacement of all PVC foams and NL25 at -40 °C, room temperature and 60 °C after a 13 J impact

Figure 16: Percentage absorbed energy of all core materials at the three operating temperatures and at 5 J, 7 J and 13 J impact energies

Figure 17: PVC foams average plateau stress as a function of strain rate along the three axis directions

Figure 18: Plateau stress at 20 % and 30 % of deformation and densification stress of NL10 agglomerated cork along the three axis direction

Figure 19: Plateau stress at 20 % and 30 % of deformation and densification stress of NL20 agglomerated cork along the three axis direction

Figure 20: Plateau stress at 20 % and 30 % of deformation and densification stress of NL25 agglomerated cork along the three axis direction

Figure A1: Split Hopkinson Pressure Bar developed at Marche Polytechnic University and used to perform the tests at high strain rates

Figure A2: Input and output force signals for the fastest tests on PVC foam (A) and agglomerated cork (B).

Figure A3: Proves of strain rate regularity for the fastest tests on PVC foam (A) and agglomerated cork (B).

Figure A4: Typical efficiency-stress curve

Figure A5: Average densification stress of the three agglomerated corks under study as a function of strain rate

Figure A6: Exemplifying plots that show strain rate sensitivity evaluation for NL10 30 % deformation plateau stress and HP 200 plateau stress.

Figure A7: Drop weight tower dynamic compressive curves of NL25cork core submitted to a 7 J impact at the three operating temperatures

Figure A8: Drop weight tower dynamic compressive curves of the HP130 core material submitted to a 13 J impact at the three operating temperatures

Figure A9: Damage of NL10 (left) and NL20 (right) samples tested at 7 J and -40 °C

Figure A10: PVC foams average densification stress as a function of strain rate along the three axis directions

Table 1:Summary of the impact energies used to evaluate core materials strain rate sensitivity through dynamic compression

Samples	2J	5J	7J	13J	30J
NL10	X	X	X		
NL20		X	X		
NL25		X	X	X	
HP130		X	X	X	
HP200		X	X	X	X
HP250		X	X	X	X

Figure 1

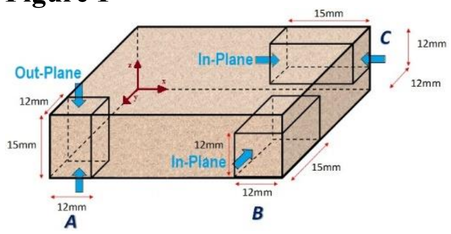

Figure 2

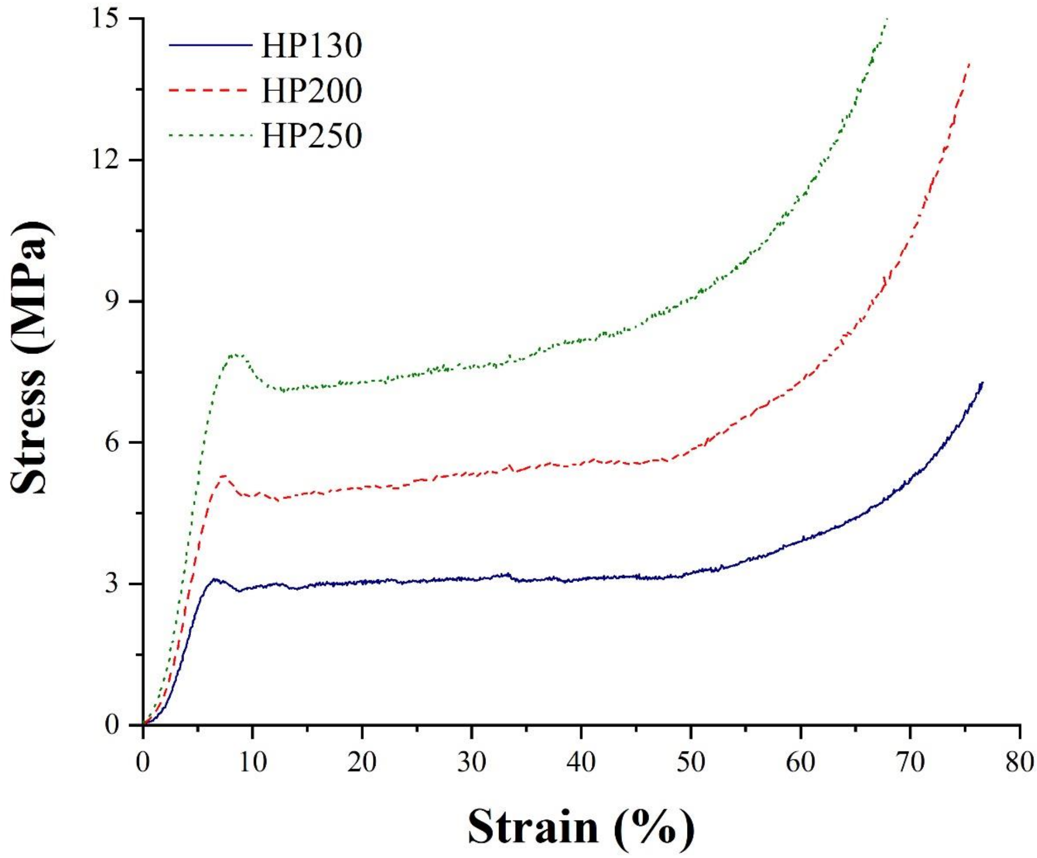

Figure 3

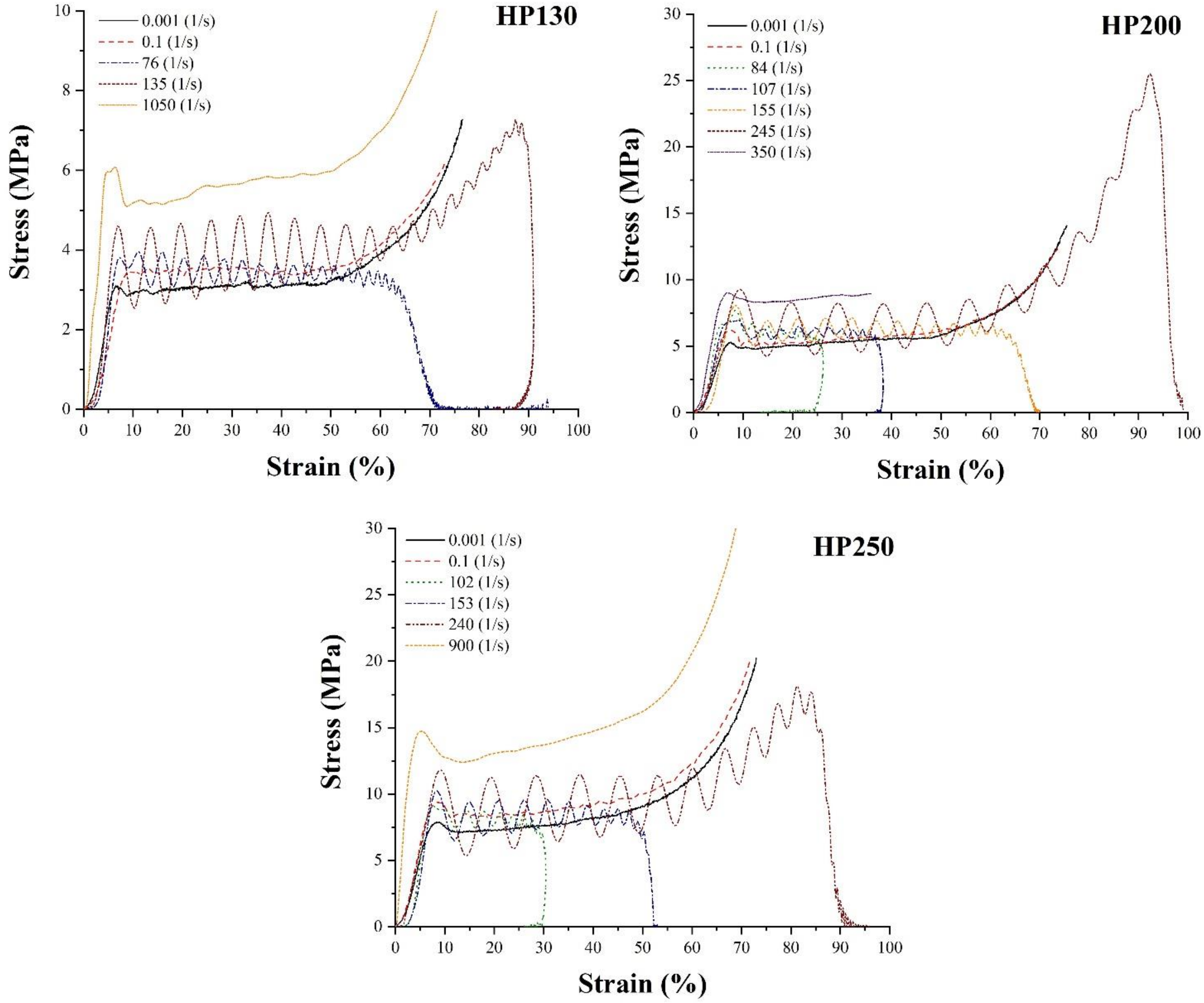

Figure 4

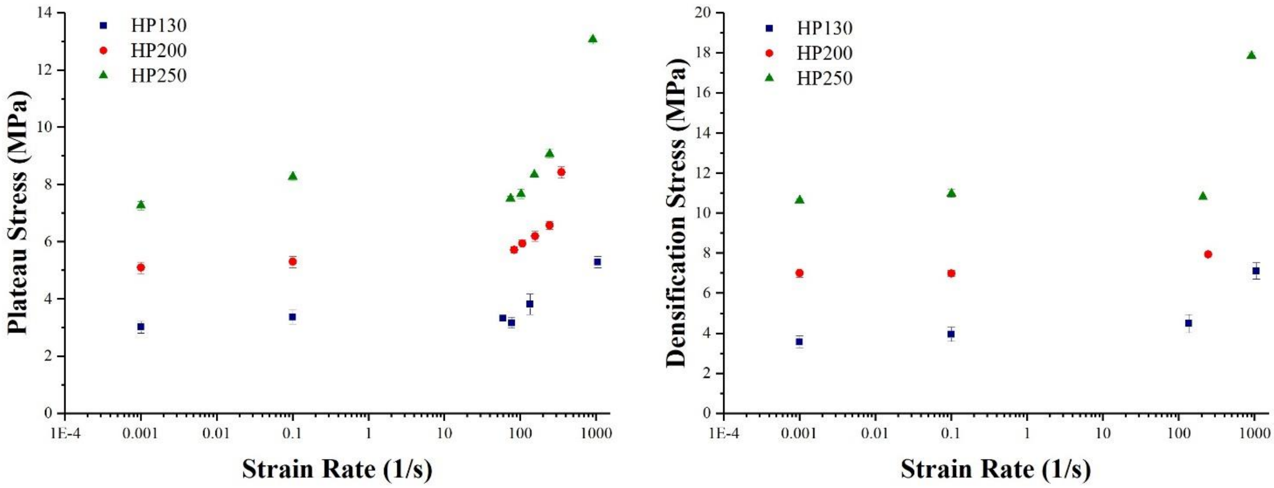

Figure 5

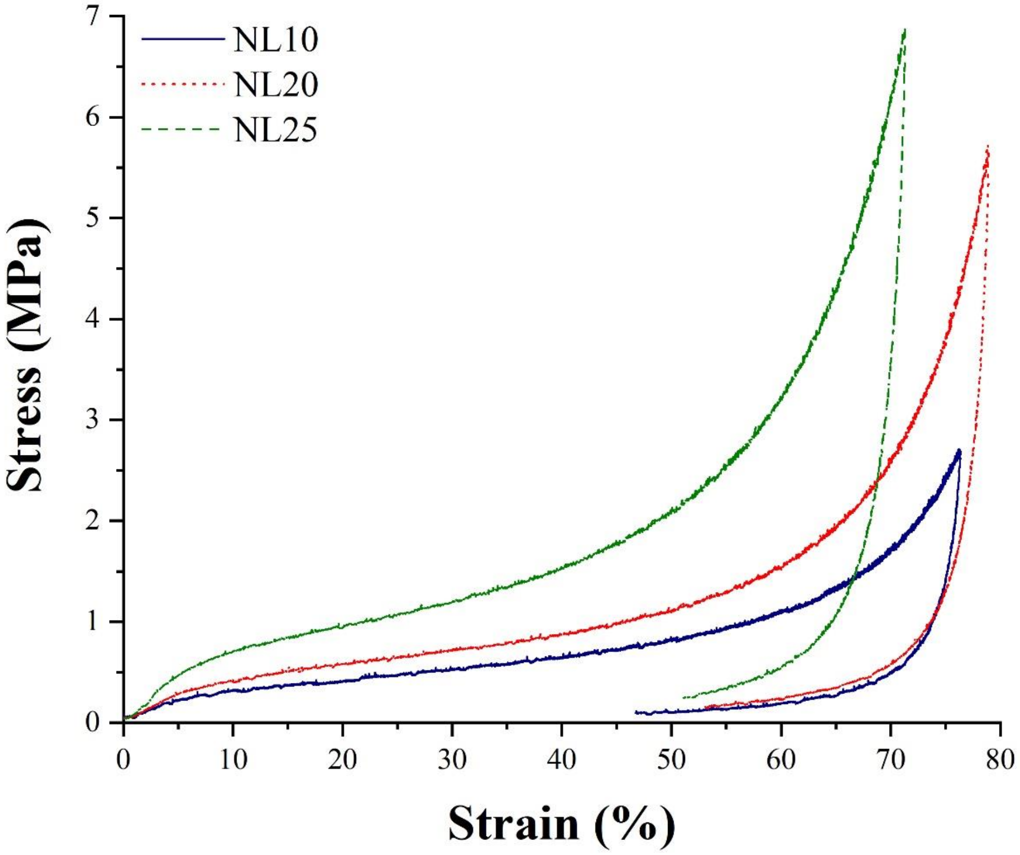

NL10
NL20
NL25
Stress (MPa)
Strain (%)
0
1
2
3
4
5
6
7
0
10
20
30
40
50
60
70
80

Figure 6

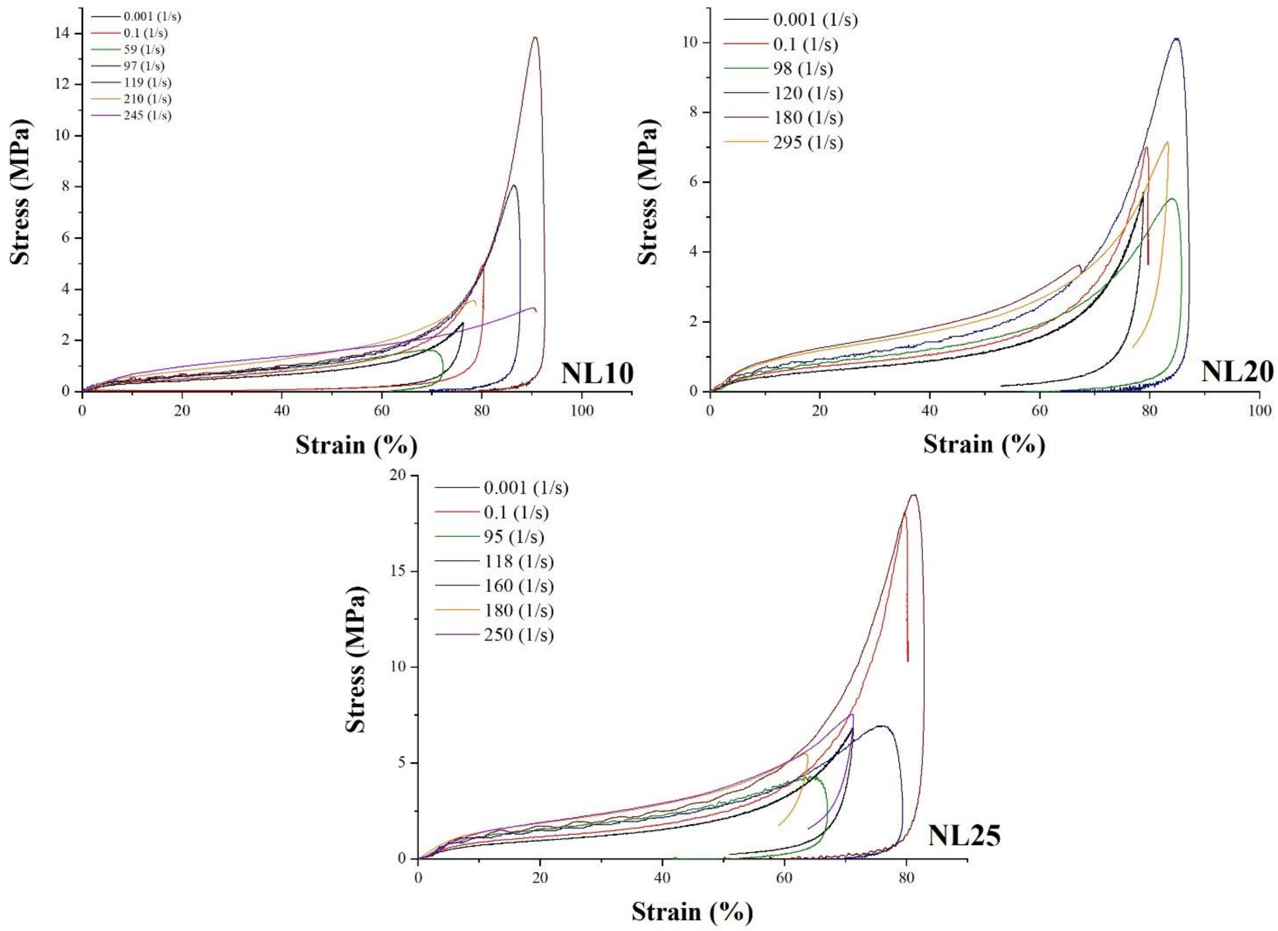
0.001 (1/s)
0.1 (1/s)
59 (1/s)
97 (1/s)
119 (1/s)
210 (1/s)
245 (1/s)
Stress (MPa)
Strain (%)
NL10
0.001 (1/s)
0.1 (1/s)
98 (1/s)
120 (1/s)
180 (1/s)
295 (1/s)
Stress (MPa)
Strain (%)
NL20
0.001 (1/s)
0.1 (1/s)
95 (1/s)
118 (1/s)
160 (1/s)
180 (1/s)
250 (1/s)
Stress (MPa)
Strain (%)
NL25

Figure 7

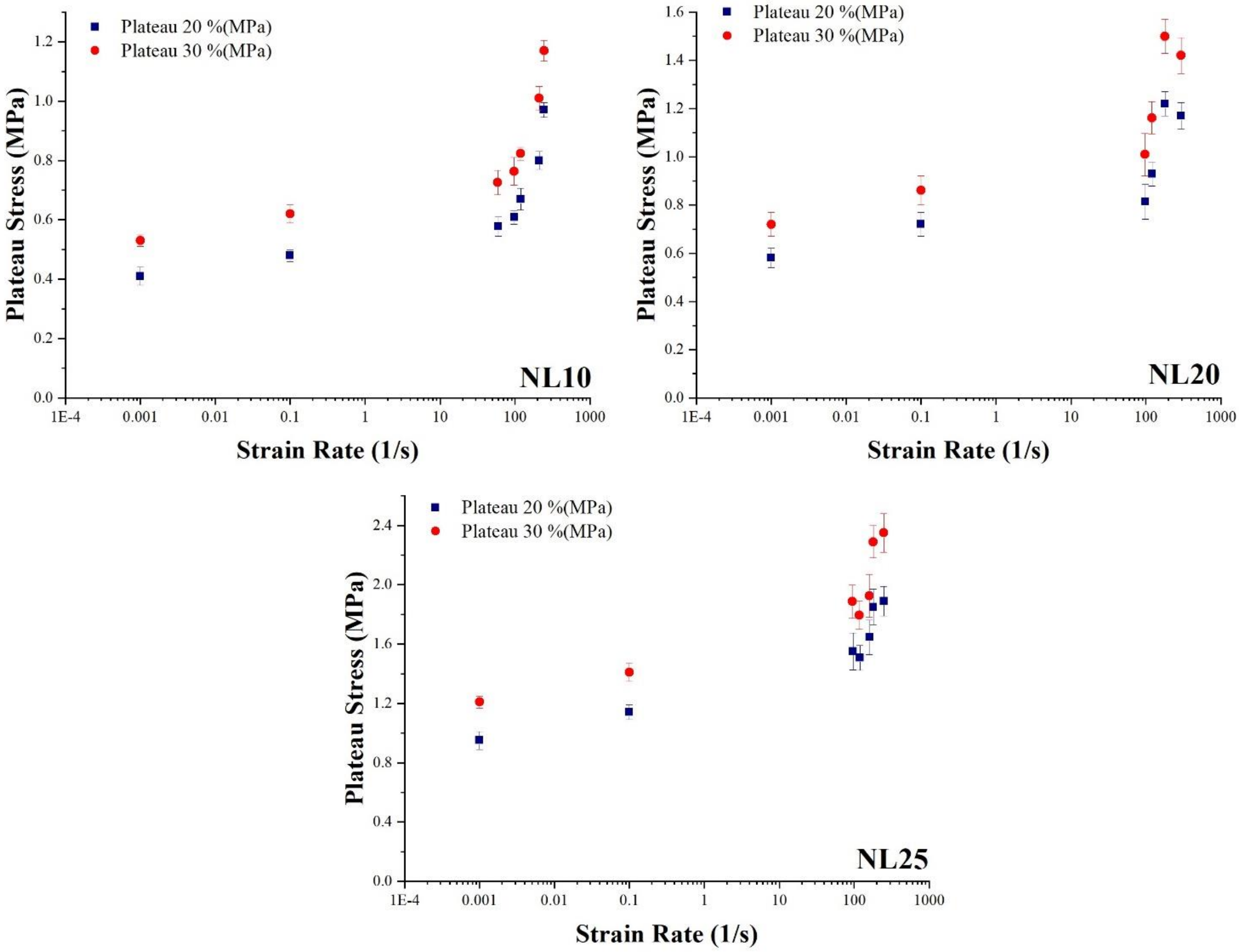

Plateau 20 %(MPa)
Plateau 30 %(MPa)
Plateau Stress (MPa)
Strain Rate (1/s)
NL10
NL20
NL25
1E-4
0.001
0.01
0.1
1
10
100
1000
0.0
0.2
0.4
0.6
0.8
1.0
1.2
1.4
1.6
2.0
2.4

Figure 8

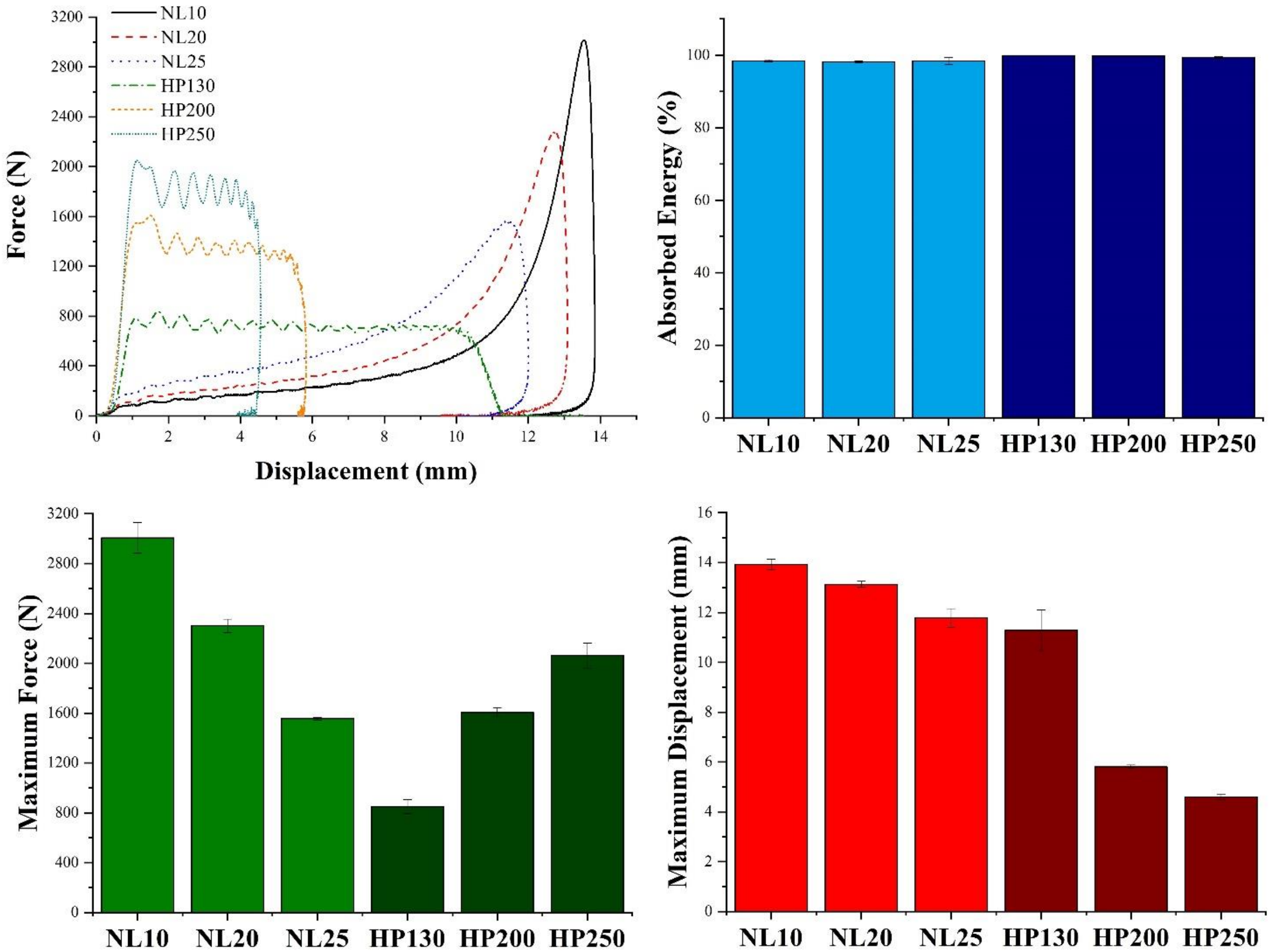
NL10
NL20
NL25
HP130
HP200
HP250
Force (N)
Displacement (mm)
0
400
800
1200
1600
2000
2400
2800
3200
0
2
4
6
8
10
12
14
Absorbed Energy (%)
0
20
40
60
80
100
NL10 NL20 NL25 HP130 HP200 HP250
Maximum Force (N)
0
400
800
1200
1600
2000
2400
2800
3200
NL10 NL20 NL25 HP130 HP200 HP250
Maximum Displacement (mm)
0
2
4
6
8
10
12
14
16
NL10 NL20 NL25 HP130 HP200 HP250

Figure 9

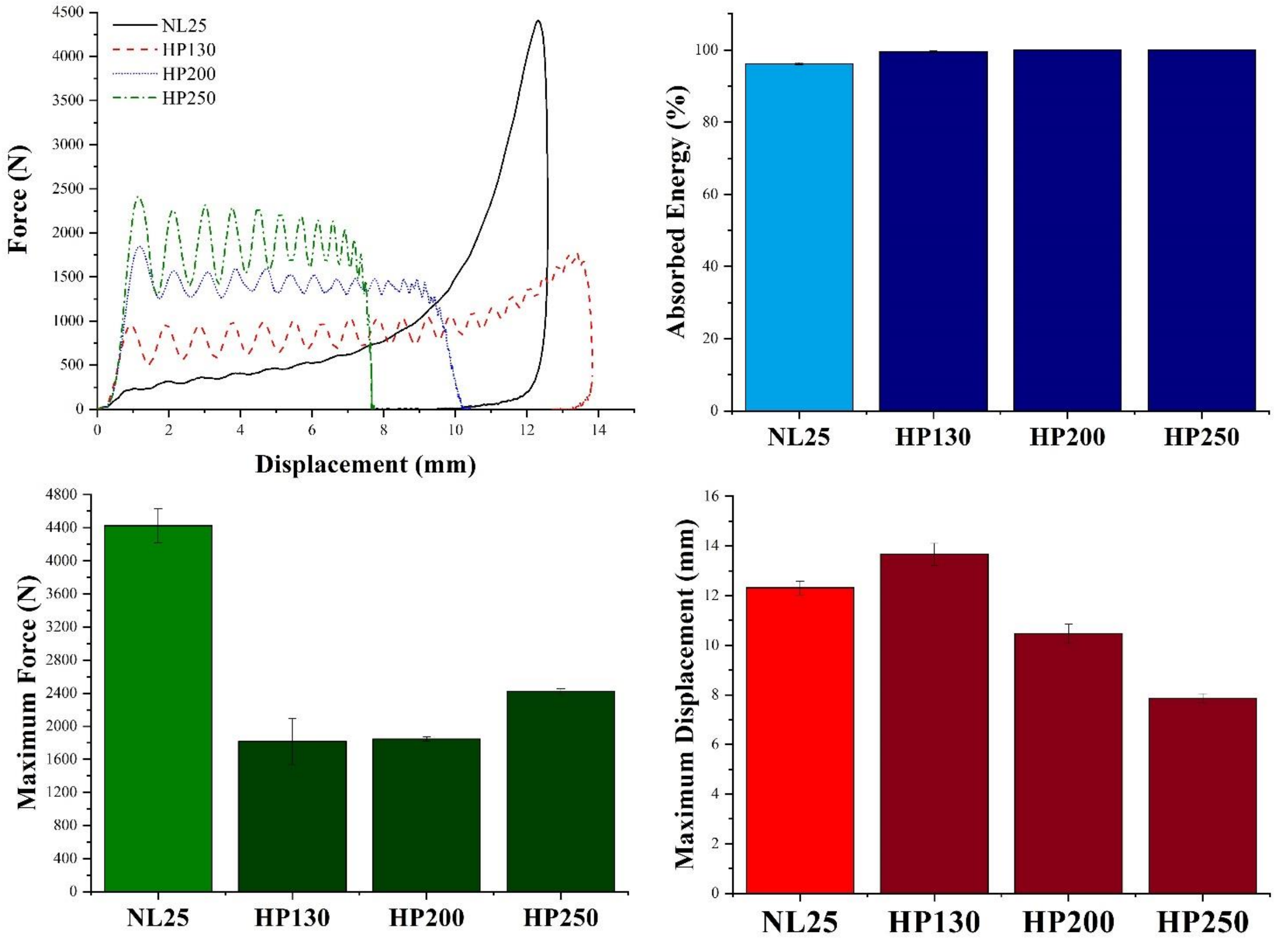
NL25
HP130
HP200
HP250
Force (N)
Displacement (mm)
Absorbed Energy (%)
NL25
HP130
HP200
HP250
Maximum Force (N)
NL25
HP130
HP200
HP250
Maximum Displacement (mm)
NL25
HP130
HP200
HP250

Figure 10

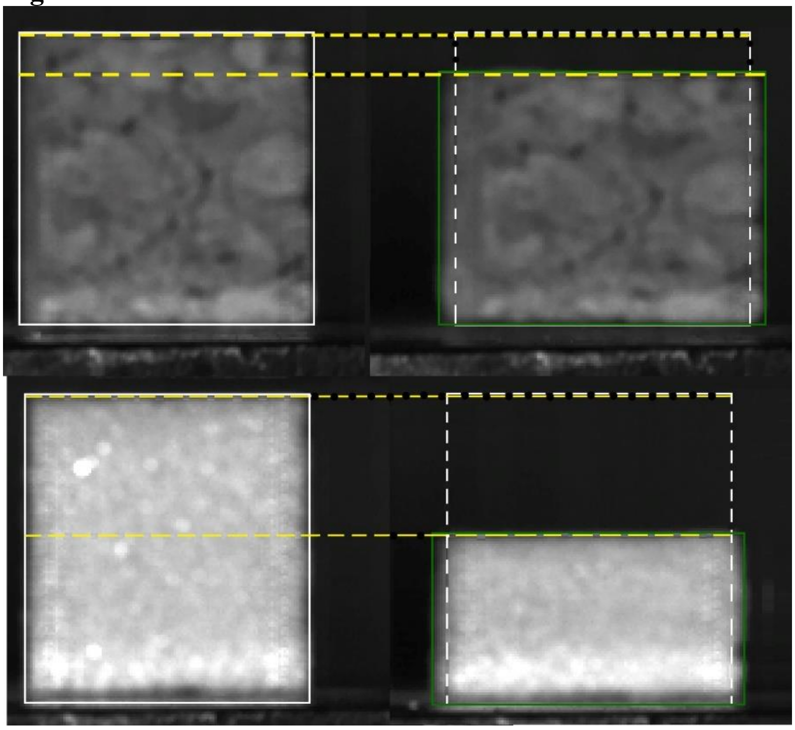

Figure 11

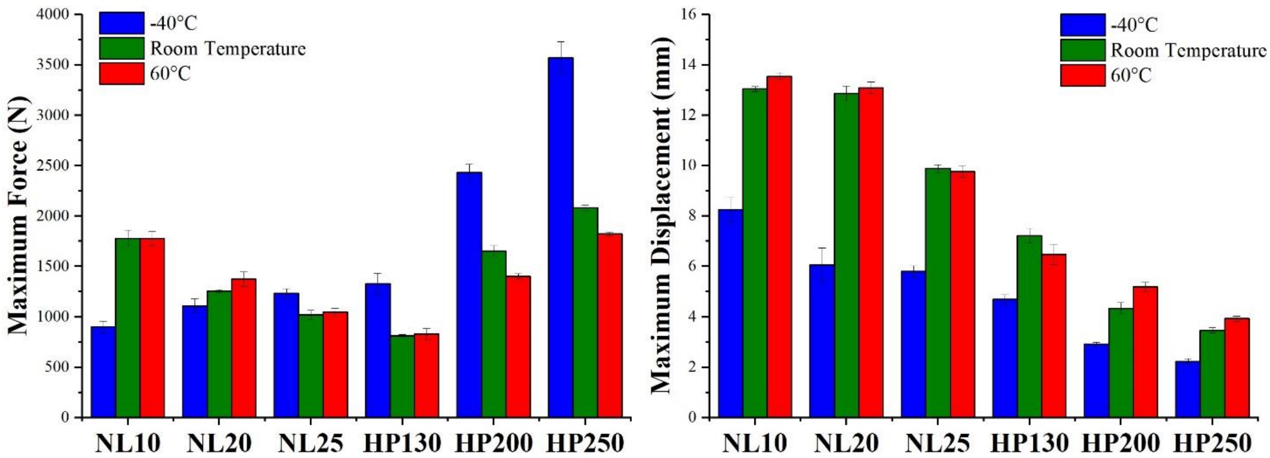

Figure12

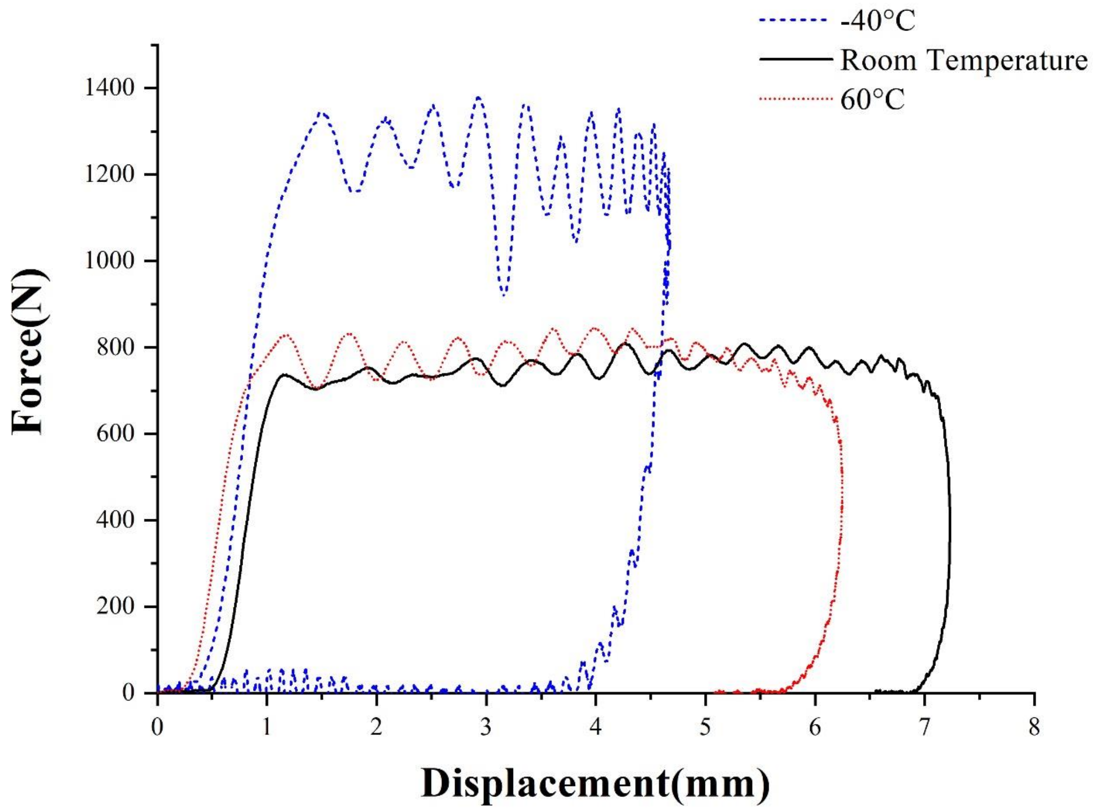

-40°C
Room Temperature
60°C
Force(N)
1400
1200
1000
800
600
400
200
0
0
1
2
3
4
5
6
7
8
Displacement(mm)

Figure 13

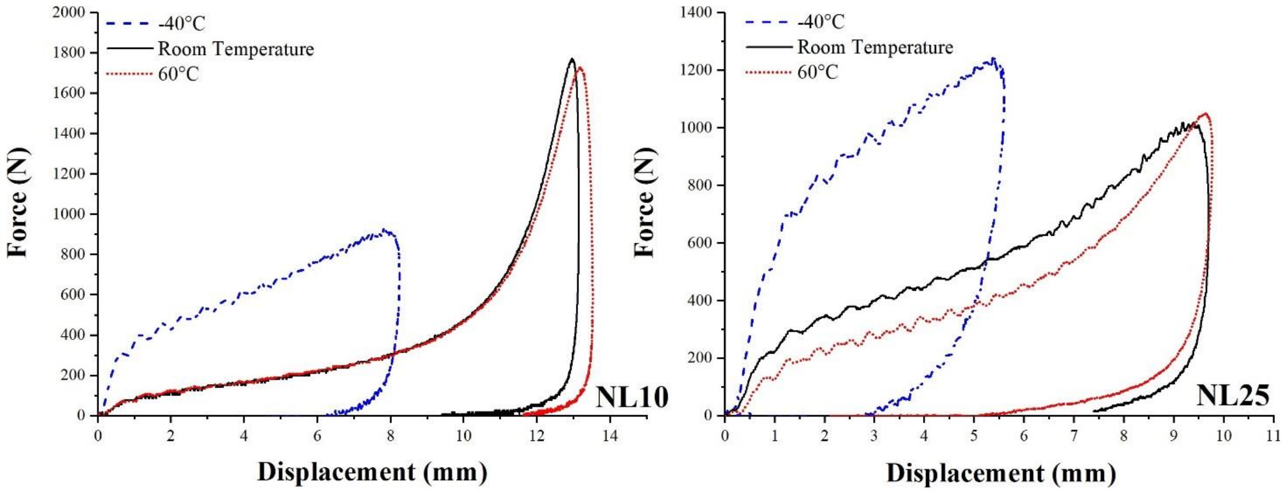

Figure 14

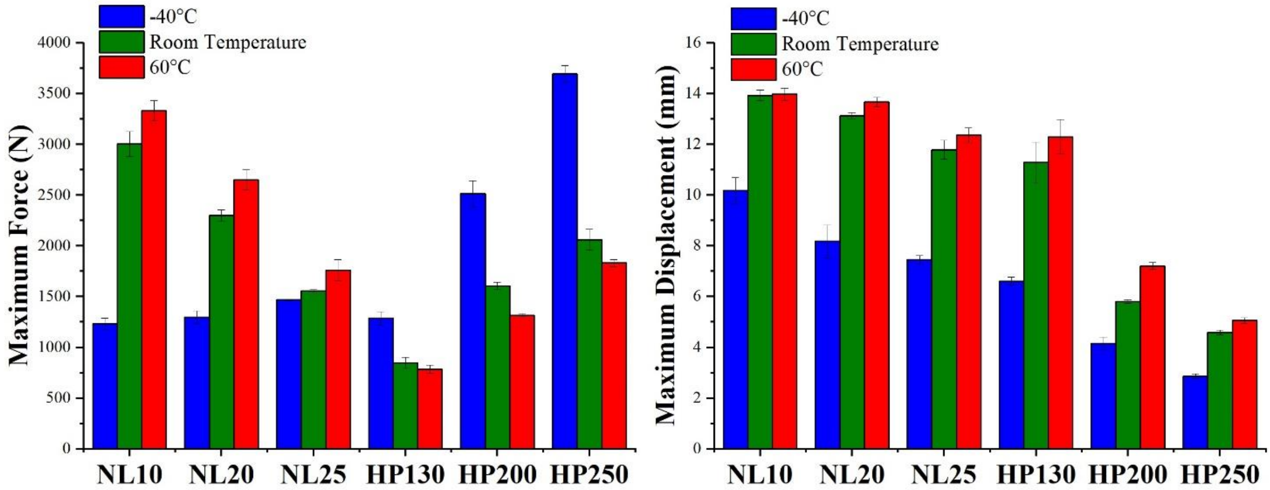

Figure 15

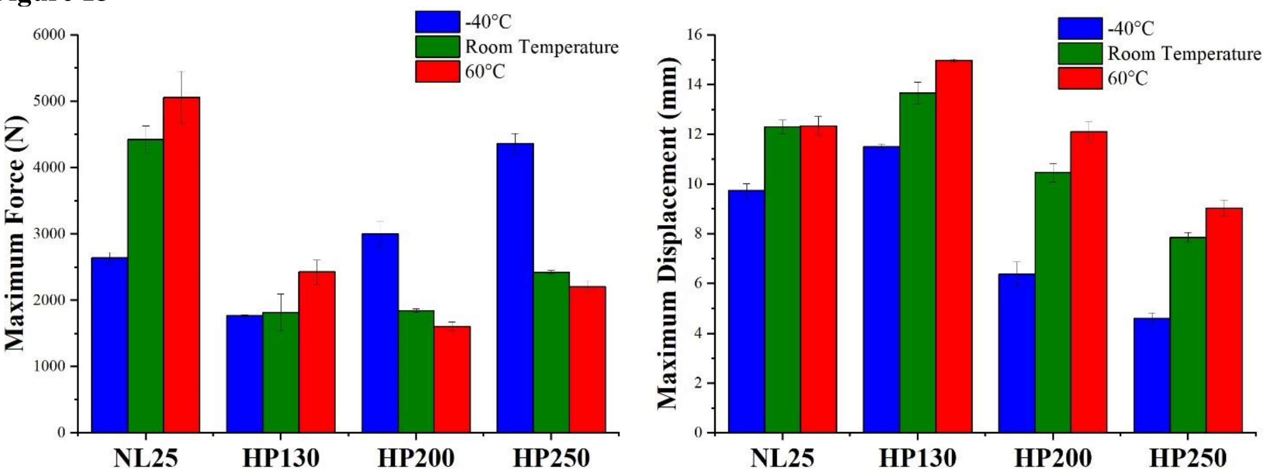

Figure 16

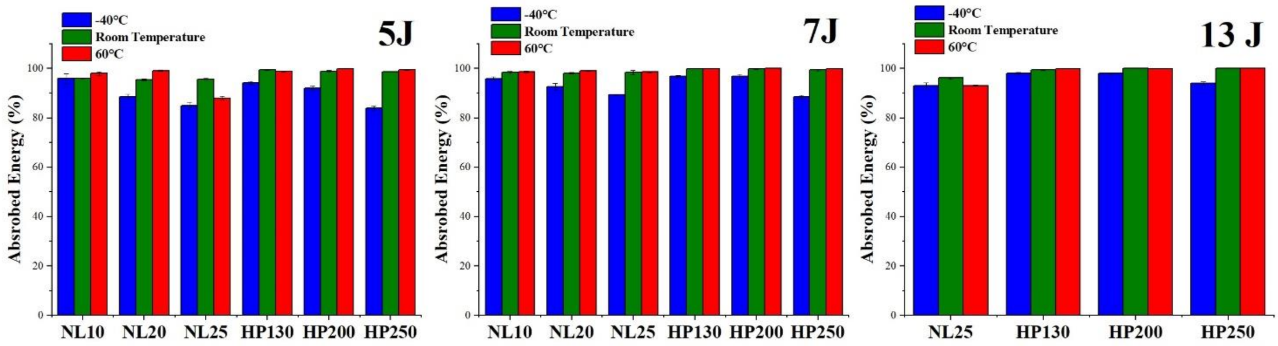

Figure 17

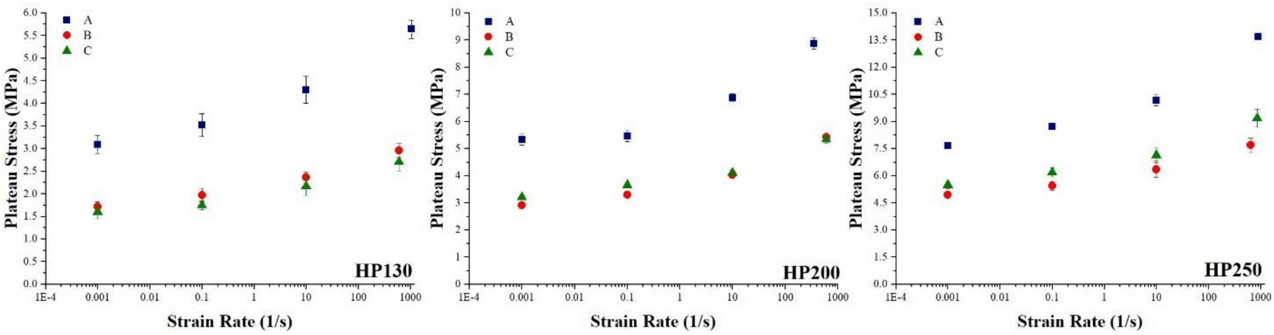

Figure 18

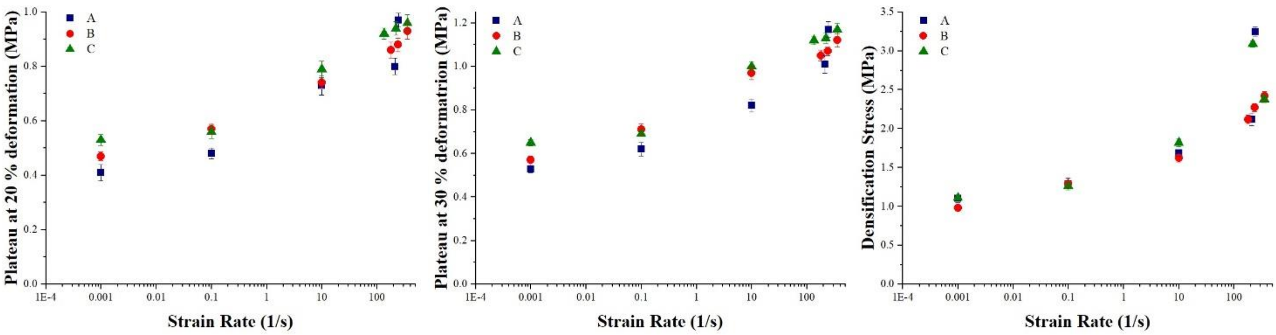

Figure 19

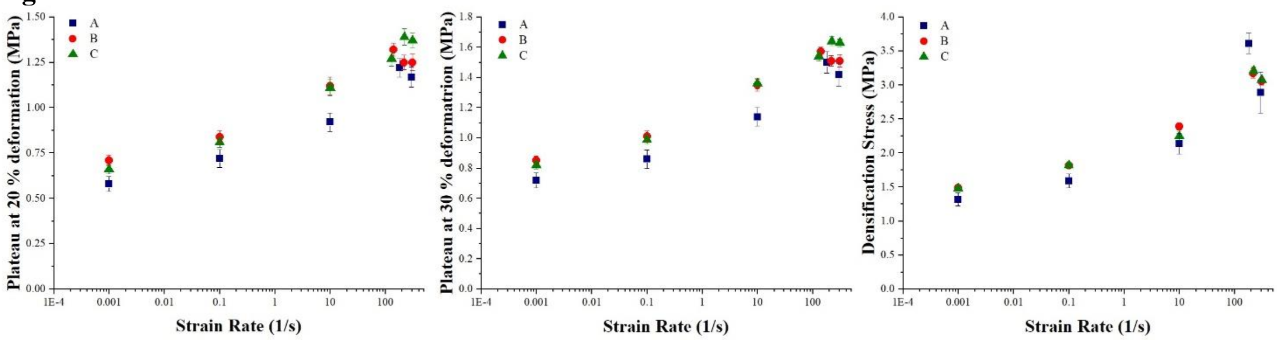

Figure 20

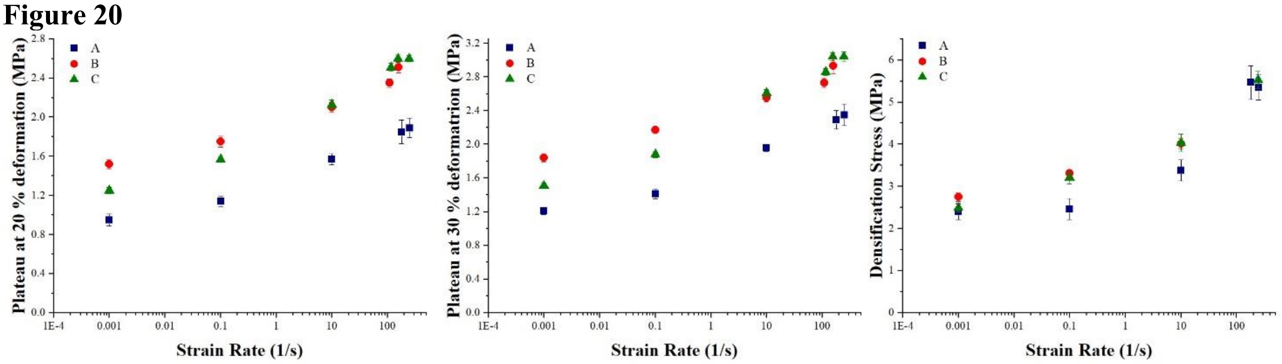

Figure A1

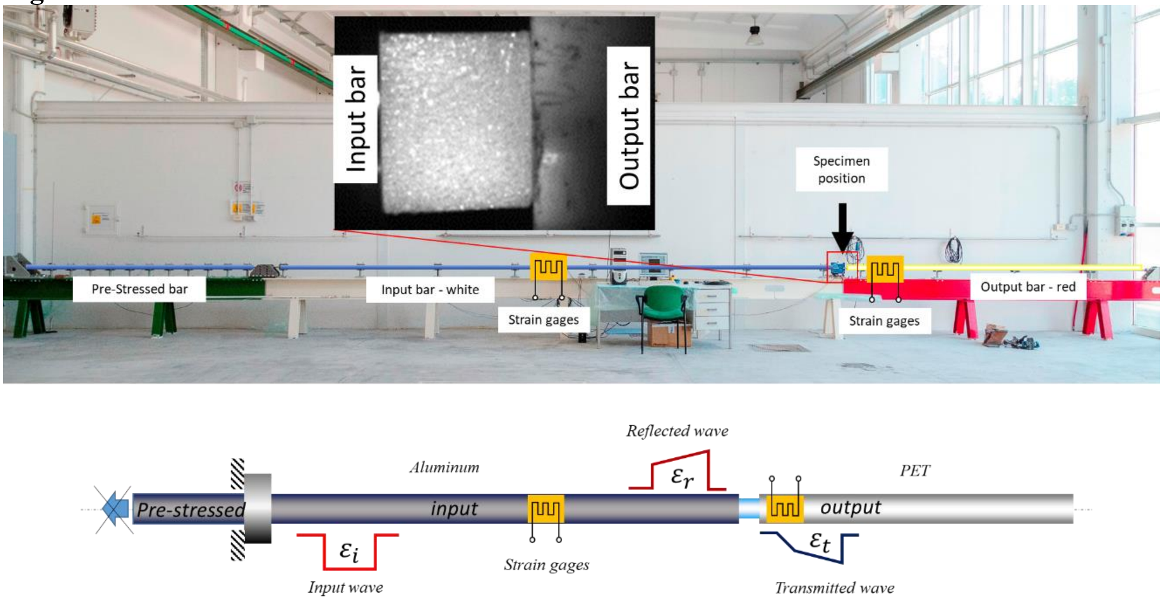

Figure A2

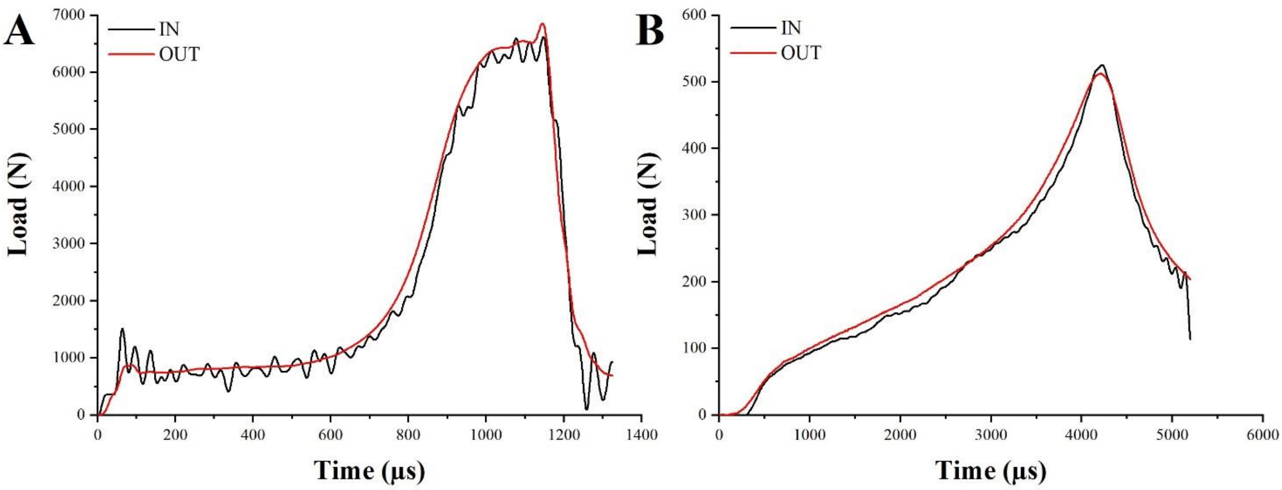

Figure A3

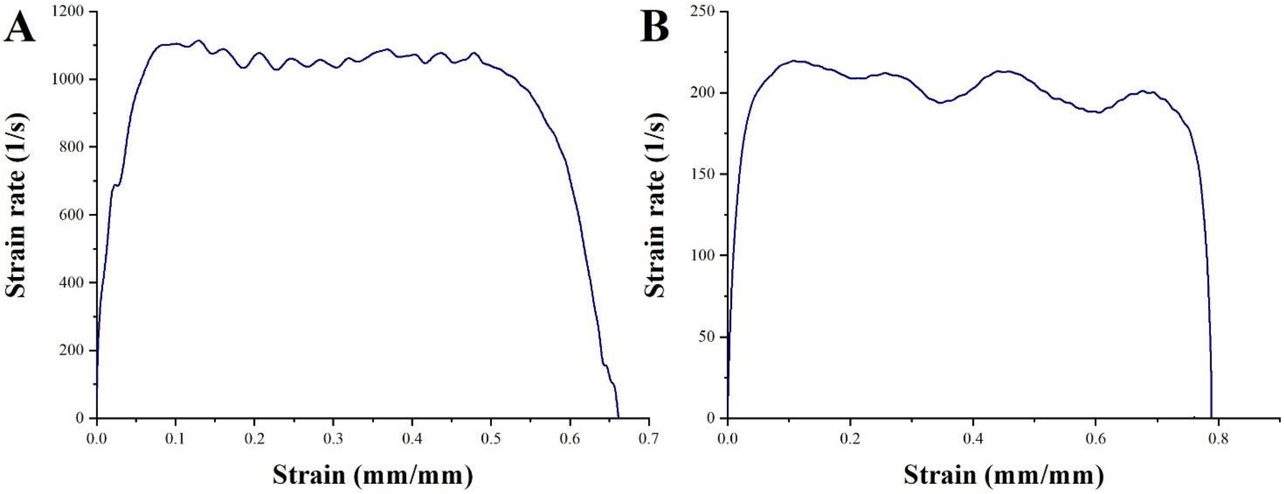

Figure A4

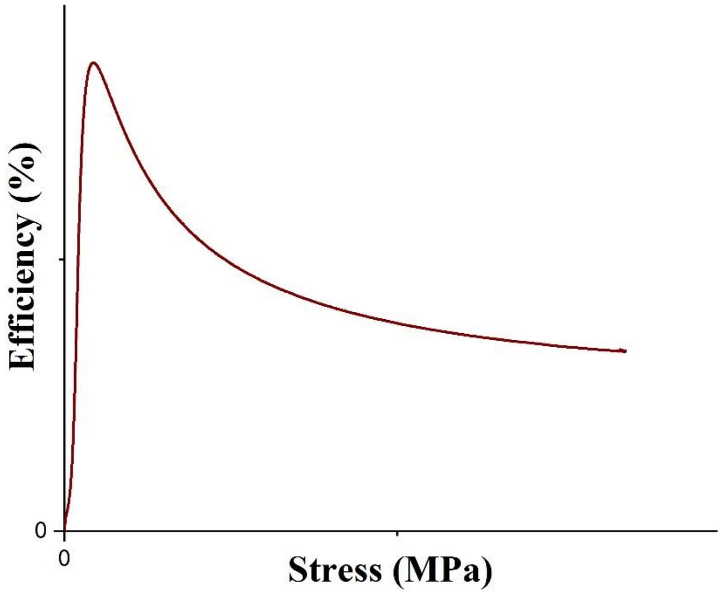

Figure A5

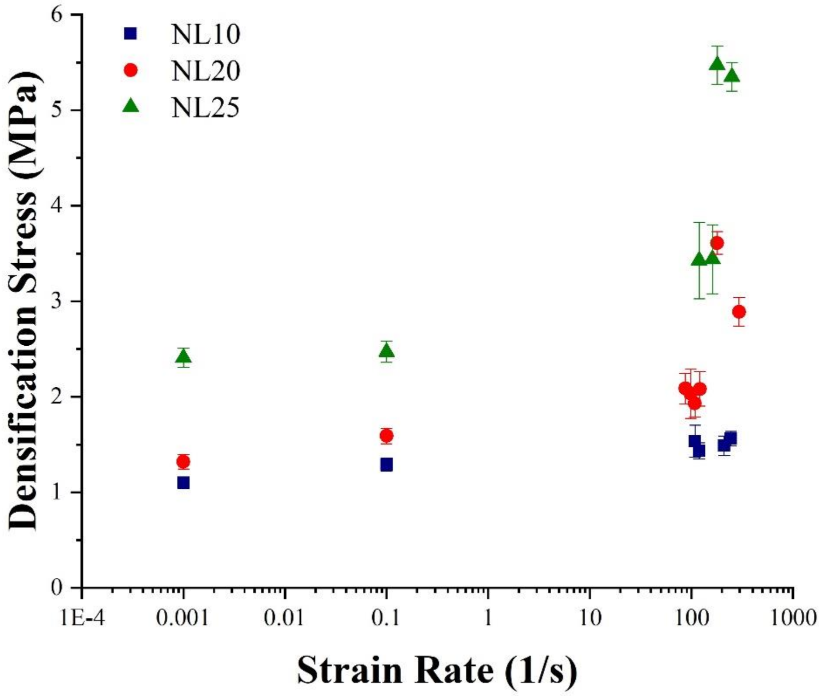

Figure A6

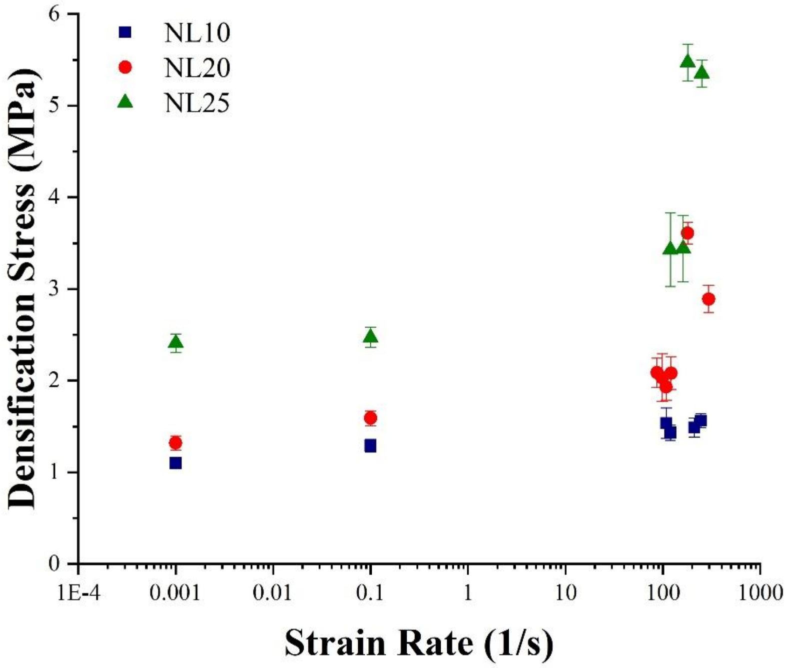

Figure A7

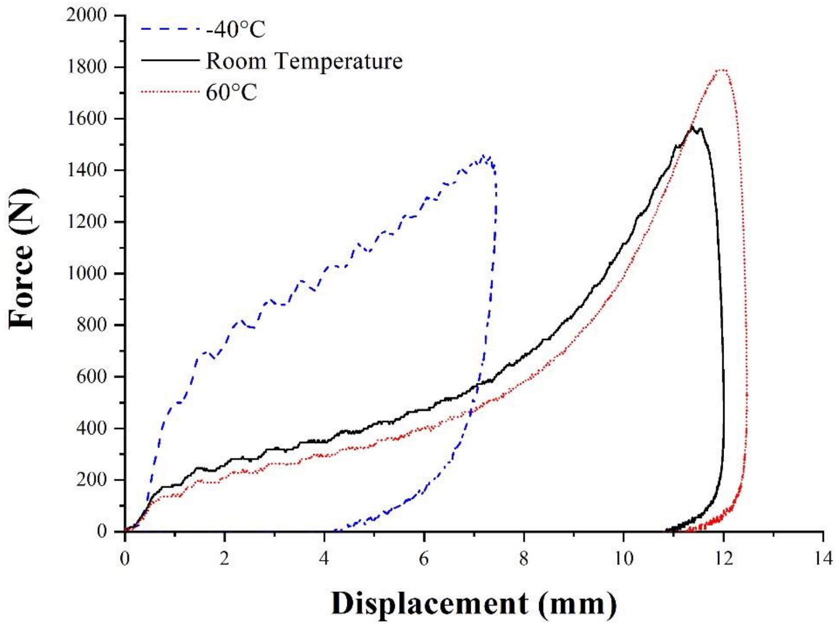

Figure A8

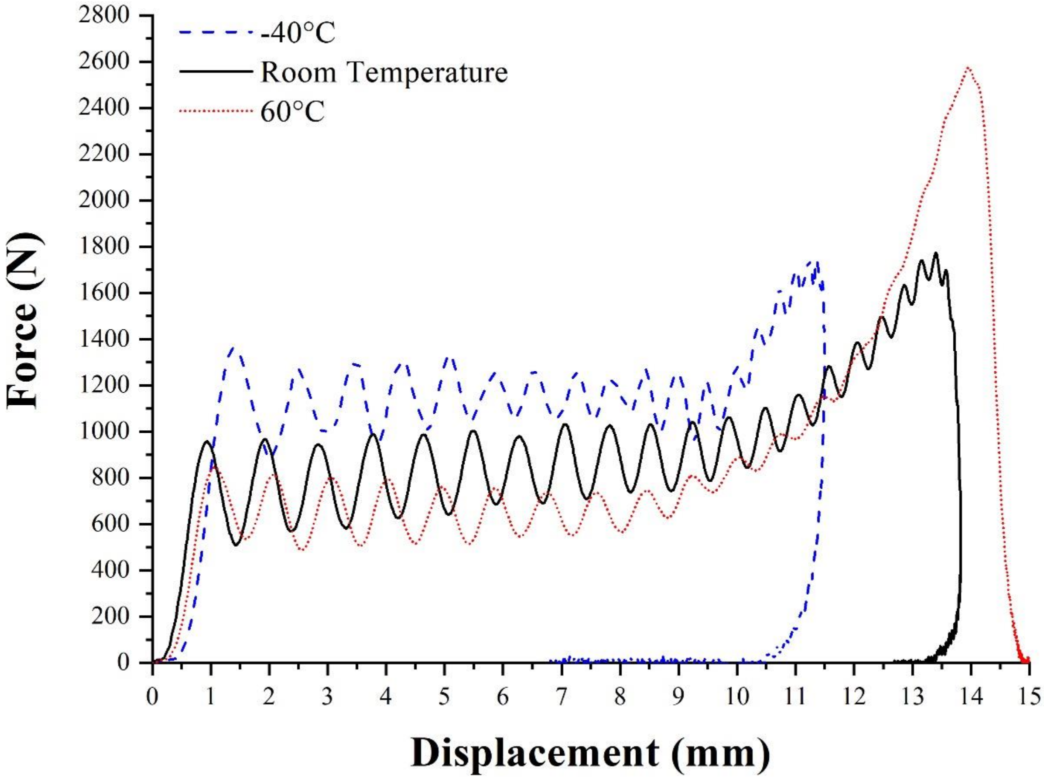

Figure A9

Figure A10

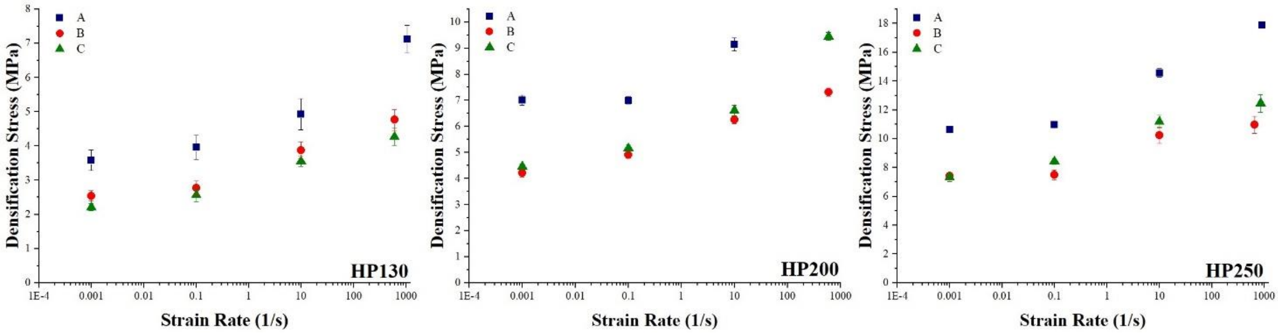

Densification Stress (MPa)
Strain Rate (1/s)
A
B
C
HP130
HP200
HP250